2018

An Investigation of Electronic Cigarette Aerosol Mixture on Craniofacial Development in Mouse Embryos

Suraj Kandalam
Virginia Commonwealth University

AN INVESTIGATION OF ELECTRONIC CIGARETTE AEROSOL MIXTURE ON CRANIOFACIAL DEVELOPMENT IN MOUSE EMBRYOS

A thesis submitted in partial fulfillment of the requirements for the degree of Master of Science at Virginia Commonwealth University.

By: SURAJ KANDALAM, B.S.

Virginia Commonwealth University, Spring, 2016

Director: Rene Olivares – Navarrete, D.D.S, Ph.D.

Assistant Professor of Biomedical Engineering

Department of Biomedical Engineering

Virginia Commonwealth University

Richmond, Virginia

June, 2018

Acknowledgments

I would like to express my deepest appreciation to everyone who supported me on this wonderful journey. First and foremost, I would like to extend my heartfelt gratitude to Dr. Rene Olivares-Navarrete, my thesis committee chairman and mentor, whose drive, expertise, and patience has truly added to my life experience. I am eternally grateful to Dr. Olivares-Navarrete for constantly holding me to my highest potential, not only in my research interests but also towards my career goals. I will always remember the micro-moments during animal surgeries that we shared. It has been a pleasure to explore this ground-breaking research on electronic cigarettes with him and I am truly excited about the futures research that will be conducted on this topic. I would also like to thank my other committee members, Dr. Chris Lemmon and Dr. Amanda Dickinson for guiding me through the intricacies of conducting formal research. I thank them for their fresh perspective on the problems I have faced throughout the process and gave me the opportunity to learn new scientific skills. I am forever grateful to Dr. Kelly Hotchkiss whose selfless support and valuable feedback kept me on track. Kelly's constant encouragement and presence helped me through my pursuit of learning. I would like to additionally thank my lab researchers, Jefferson Overlin and Kegan Sowers, who were always willing to lend a helping hand whenever needed. Finally, I would like to thank my parents, my brother, my sister-in-law, my adorable niece and nephew for their everlasting support and love which helped me be successful in this endeavor.

Table of Contents

List of Tables

List of Figures

Abstract

AN INVESTIGATION OF ELECTRONIC CIGARETTE AEROSOL MIXTURE ON CRANIOFACIAL DEVELOPMENT IN MOUSE EMBRYOS

Suraj Kandalam, B.S.

A thesis submitted in partial fulfillment of the requirements for the degree of Master of Science at Virginia Commonwealth University.

Virginia Commonwealth University, 2018

Major Director: Rene Olivares-Navarrete, D.D.S, Ph.D., Assistant Professor, Department of Biomedical Engineering

E-cigarette (e-cig) use has increased in recent years among teenagers and young adults. From 2011 to 2015, e-cig use has increased by 900% in this demographic. E-cigs are battery powered nicotine delivery systems that vaporize e-liquids, a solution composed of propylene glycol (PG), vegetable glycerin (VG), nicotine, flavoring, and coloring agents. While cigarettes are associated with a wide range of complications in fetal development, including craniofacial malformations, the effects of e-cig use during pregnancy are not known. The aim of this study was to determine the effects of exposure to e-cig aerosol mixtures (e-cigAMs) on proliferation, migration, and differentiation of neural crest cells (NCCs) *in vitro* and craniofacial development in mouse embryos *in vivo*. E-cigAM was produced by bubbling e-cig aerosol into saline. E-cigAMs were generated for unflavored (Research Grade) e-liquid consisting of 70:30, 30:70, or 15:85 PG:VG ratio as well as flavored e-liquid such as Almond Butter, Pineapple and Coconut, and Strawberry Shortcake. Murine cranial NCCs were cultured in complete embryonic stem cell medium. Metabolic activity, gene expression, migration, and proliferation experiments were performed after 7d of exposure. For *in vivo* studies, osmotic pumps loaded with e-cigAM

were implanted into 10 week-old female mice, which were mated 7 days later. Embryos were harvested after 17.5 days of development. Embryos were fixed and imaged on a high-resolution μCT scanner (n=10/treatment). Following three-dimensional reconstruction of images, craniofacial morphometry was characterized using generalized Procrustes analysis and discriminant function analysis. *In vitro,* metabolic activity was reduced in all treated groups, and e-cigAMs with nicotine exhibited the strongest effect. NCC migration and proliferation were inhibited by e-cigAM in a VG and nicotine dose-dependent manner. E-cigAM inhibits neural crest cell proliferation dependent on PG/VG ratio and nicotine dependence. E-cigAM exposure also attenuated the expression of genetic markers of angiogenesis, chondrogenesis, osteogenesis and smooth muscle**.** *In vivo,* e-cigAM exposure generated shape changes including narrowing and shortening of the orofacial area along aplasia of the eye and midface hypoplasia. The results indicate that fetal exposure to e-cigAM alters craniofacial development.

Chapter 1 – Introduction/Overview

Cigarette smoking is estimated to cause more than 480,000 deaths annually and is the leading preventable cause of death in the United States [1]. Though cigarette consumption continues to decrease nationally, there has been an increase in electronic cigarette (e-cigs) use, particularly among young people. This increase in e-cig use can be attributed to the perceived notion of e-cigs being “safer” than traditional cigarettes.

E-cigs are battery-powered nicotine delivery systems that vaporize e-liquid, a solution primarily composed of propylene glycol (PG), glycerol or vegetable glycerin (VG), nicotine, flavorants, and colorants [2]. They come in a variety of products ranging from first generation to the current models being used today along with a wide range of e-liquids (Figure 1). E-cigs have several different components that work in unison such as a battery, a reservoir which holds the e-liquid, an atomizer (heating element) and a mouthpiece through which the user inhales the vaporized e-liquid (Figure 2).

Currently there are more than nine million adult vapers in the United States. More than two million youth in the US have used an e-cig device in the last 30 days [3]. Since 2011, there has been a 900% increase in e-cig use within the young population. While cigarettes are associated with a wide range of complications in fetal development including craniofacial malformations, the effects of e-cig use during pregnancy is unknown.

Craniofacial tissues like facial bones, cartilage, teeth, and vasculature are formed after gastrulation, in large part by neural crest cells (NCCs). These tissues are sensitive to drugs such as nicotine, which impairs NCC activity and causes craniofacial defects in the developing embryo. Successful NCC proliferation, migration, and differentiation are

critical to the normal formation of craniofacial tissues. Therefore, compounds that alter NCC behavior may affect craniofacial development [4].

This study aimed to determine the effects of exposure to e-cigarette aerosol mixtures (e-cigAMs) on the differentiation, proliferation, and migration of NCCs *in vitro* and on craniofacial development of mouse embryos *in vivo*.

Chapter 2 – Background/Literature Review

History of Traditional Cigarettes

E-cigarettes are not the first or last alternative tobacco product advertised as less harmful than cigarettes. Throughout history there are multiple tobacco products that have been created to reduce the harm of tobacco in public health. In order to understand the role of current e-cigarettes on public health, it is imperative to comprehend the role of its derivatives such as nicotine delivery, the multiple “reduced harm” tobacco products advertised, and the impact of these tobacco products on the public’s health.

Since the advent of cigarettes, manufacturers, scientists, entrepreneurs, and public health leaders have proposed for modifications to make them less harmful. Nicotine delivery was of utmost importance in the early developmental stages of cigarettes as a way to retain consumers. From 1913 – 1918, several cigarette companies such as Camel, American Tobacco, and Lucky Strike all reformulated their cigarettes to make them more palatable. Advertisements in the mid-1900s popularized cigarettes by makes claims such as, “Smoking Camels stimulates the natural flow of digestive fluids … increase alkalinity” [5]. Overall, companies made early modifications to cigarettes to make it seem more palatable, with higher nicotine delivery and uptake, and finally marked as “safe” than the unmodified cigarette.

Background on E-cigarettes

The earliest appearance of the e-cigarette appeared in 1963 as a US patent application by Herbert A. Gilbert. Gilbert aimed to create a “smokeless, non-tobacco cigarette” that was a safer alternative to smoking in general. The first working prototype was developed by a Chinese pharmacist, Hon Lik, in 2003. It was later introduced to the

US market in 2007. The usage rate has increased since then especially among the youth and young adult population. This increase in popularity among the youth population is due to the widespread advertising (TV commercials, print advertisements, and social media) similar to that of traditional cigarettes. Currently there are many different versions of e-cigarette ranging from first generation “cigalikes” to third generation models such as “e-cig tanks and mods”. E-cigs are a class of electronic nicotine delivery systems (ENDS) that vaporize e-liquid, a solution primarily composed of propylene glycol (PG), glycerol or vegetable glycerin (VG), and nicotine, flavorants, and colorants. E-cigs are composed of a battery, a reservoir for holding e-liquid, an atomizer (heating element), and a mouthpiece through which the user puffs.

Prevalence of E-cig use Among Youth and Young Adult Population

It is imperative to understand the trends of e-cig use among our youth to fully understand the benefits/harms of these new tobacco products. Since 2011, there has been an astounding 900% increase in e-cigarette use among just our youth (high school and middle school students) in the United States [5]. Currently, e-cigs are the most commonly used tobacco products among high school students. In 2016, approximately more than two million middle and high school students used e-cigarettes. In a 2014 survey conducted in study, 81% of current youth e-cig users alluded to the appealing flavors as the primary reason for use. Among adults who had never smoked cigarettes, young adults between 18-24 years of age showed the highest trends in ever e-cigarette use (Figure 3). In other words, one in every ten never-smokers between the ages of 18-24 had ever tried an e-cigarette at least once [6]. This statistic is alarming because it shows that young people of reproductive age are the primary users.

The Role of Neural Crest Cells in Craniofacial Development

Neural crest cells (NCCs) differentiate into many different cell types and tissues in the body in addition to connective tissues, chondrocytes, and myofibroblasts. Due to the pluripotency of NCCs, they are sometimes referred to as the “fourth” germ layer [7] They arise from the ectoderm layer around the neural tube during neurulation of embryogenesis. Their main contribution is in the face, specifically the facial skeleton and facial connective tissue that is derived from cranial NCCs. Cranial neural crest cells that migrate dorsolaterally are responsible for the formation of the craniofacial mesenchyme that produce the cartilage, bone, cranial neurons, glia, and connective tissue of the face [7]. Consequently, genetic diseases that occur in the craniofacial region can be attributed to any abnormalities that occur during NCC generation, migration, proliferation, and differentiation. To understand any craniofacial abnormality, it is essential to first understand the development of NCCs derivatives in the face.

Normal craniofacial morphogenesis includes interactions between the NCCs and other cell populations in close proximity. Seven prominences make up the embryonic vertebrate face: the singular frontonasal (FNP), the paired lateral nasal, and maxillary and mandibular prominences. Specifically, the FNP is responsible for the formation of the forehead, middle of the nose, upper lip, philtrum, and primary palate. Both the maxillary and mandibular prominences are derived from the first pharyngeal arch. These complex interactions between NCCs and its neighboring cell populations have a profound effect on craniofacial development; consequently, this complex interaction can also lead to many malformations [8],[9].

Shape Analysis Method: Geometric Morphometric Analysis and Procrustes Analysis

Shape analysis methods of geometric morphometrics and Procrustes analysis were used to analyze murine embryos in this study. Shape analysis plays a very important role in a variety of biological studies that produce differences in shape between individuals and/or their parts. Some biological processes that produce shapes changes are disease or injury, ontogenetic development, etc. As always, these differences in shape changes suggests abnormalities in functional roles, differences in growth and morphogenic development, and a variety of other processes. These comparisons are valuable because they help biologists to visualize unfamiliar but meaningful biological components of shape. Unfortunately, qualitative comparisons at best are very relative and specific to the individuals that are being compared. Characterizing craniofacial structures requires advanced shape analysis tools that can visualize and analysis the subtle changes in these structures. When precision is needed, a more quantitative approach is needed such as geometric morphometrics.

Geometric morphometrics (GM) is the analysis of shape using a quantitative approach. GM methods consists of a multivariate analysis that offers precise and accurate description to help us visualize differences among complex shapes. This analysis is performed by acquiring landmarks and semi-landmarks and implementing an ordination technique called Procrustes superimposition in order to perform principal component analysis (PCA), and discriminate function analysis (DFA). Before any of these analyses are conducted, we must first define what “shape and size” is in the field of geometric morphometrics.

In GM, shape is defined as “all the geometric information that remains when location (translation),scale and rotational effects are filtered out from an object” [10]. Kendall implied that by removing the differences between configurations of location, scale, and orientation of an object, the only characteristic that is left is shape. Kendal’s definition of size says, “scale is the definition of size that is complementary to shape” [11]. In GM, size is determined by computing the square root of the sum of all squares of each distances of all the landmarks from the center of its object (centroid). The centroid size is mathematically independent of its size. Procrustes analysis performs all the shape and size variables that were aforementioned.

Procrustes superimposition analyzes objects by translating, rotating, and scaling them around the origin to obtain shape coordinates and Procrustes distances. Procrustes minimizes the differences between landmark configurations. Since geometric shape variables are neither biologically and or mathematically independent, another ordination method called principal component analysis (PCA) is used. These shape variables are correlated in way that describe the organism functionally, developmentally, and also genetically. PCA makes these patterns simplified and easier to interpret by replacing these shape variables with principal components that are liner combinations of the original variables and independent of each other. It is important to keep in mind that PCA compares individuals, rather than groups. Canonical variate analysis (CVA) is another type of ordination method that analyzes these organisms by group. In other words, CVA simplifies the differences seen among group means. Discriminant function analysis (DFA) is a type of CVA but only compares differences between two groups only. DFA is mostly used when comparing a single group to the control group to see an effect.

Chapter 3 – An Investigation of Electronic Cigarette Aerosol Exposure on Neural Crest Cells and Craniofacial Abnormalities in a Mouse Model

Introduction

Smoking cigarettes is estimated to cause more than 480,000 deaths annually and is the leading preventable cause of death in the United States [5]. Although cigarette use is on the decline, there has been an increased popularity of electronic cigarettes (e-cigs), notably among youth and non-smokers [3]. Currently, there are more than two million young adults in the United States, including women of reproductive age, who have used an e-cig device in the last 30 days [3]. This growth in e-cig use may be due to advertisements from the public media and the perceived safety of e-cigs compared to cigarettes.

E-cigs, despite their name, function entirely different from cigarettes, using propylene glycol (PG), vegetable glycerin (VG), and water as aerosolized carrier solvents for flavor, coloring agents, and nicotine delivery [2]. E-cig aerosols, produced by heating and aerosolization of e-cigarette liquids, contain nicotine, aldehydes, phenols, heavy metals, and other volatile organic compounds in varying quantities. Differences in the manufacturing process, user-tunable properties such as device wattage, and improper operation of e-cig devices lead to variation in the quantity of these compounds in the resulting aerosol [12]. Since e-cigs have opened in market, scientific research has only been limited to their effect on the cardiovascular and lung regions.

Several studies have shown the acute effect of e-cigs on the cardiovascular system, such as changes in blood pressure levels, high heart rate, arterial stiffness, and oxidative stress [13]. Though there is limited research on the short and long-term effects of e-cig

delivery systems, research has shown that exposure of the lung to various components of e-cig aerosol (flavorings, vapor particulants, etc) could potentially damage the respiratory system or worsen existing conditions. A study from John Hopkins University found significantly high levels of toxic metals (cadmium, chromium, lead, manganese, and nickel) in the vaporized e-liquids from cig-a-like devices [14]. A follow up study with current mod-tank devices resulted in similar results, suggesting that metals from e-cigarette heating coils may leak into the vaporized e-liquid [15]. Both of these studies signify that chronic inhalation of these toxic metals have been related to liver, cardiovascular, and even carcinogenic effects in the body. It is imperative that more research is conducted, especially in the developmental and reproductive stages, due to the alarming rate of young reproductive age women that use e-cigs. The two most common perceptions of e-cig use in pregnancy were identified as: e-cigs are safer and a potentially healthier alternative (for mother and baby) compared to traditional cigarettes and e-cigs are used as a tool for smoking cessation [16], [17]. It is well known that cigarette use during pregnancy is associated with a wide range of fetal complications, including intrauterine growth restriction, prematurity, susceptibility to infant respiratory disease, altered nervous system development, and craniofacial malformations [18]–[20]. These complications are known to be the result of various components of cigarette smoke: nicotine, carbon monoxide, and products of the organic combustion [21], [22].

Some e-cig aerosol components are present in cigarette smoke as well and have been identified as mediators of the fetal complications of smoking in various animal models. In a fetal mouse model, Ozturk et al. demonstrated that nicotine exposure *in utero* leads to improper palatal fusion and persistence of the midline epithelial seam [23]. In zebrafish,

propylene glycol exposure produced smaller larvae with fewer somites; behaviorally, these larvae exhibited altered swimming behavior and more spontaneous contractions. Our previously published work involved a *Xenopus laevis*, a craniofacial animal model, and a mammalian neural crest cell line to test the effects of several aerosolized e-liquids (e-cigAM) [24]. E-cigAM exposure during embryonic development of embryos showed various craniofacial defects such as median facial clefts and midface hypoplasia. Additional analysis disclosed cranial cartilage, muscle defects and a reduction in the blood supply to the face. Quantitative analysis of facial morphology indicated that nicotine concentration was not the prominent contributor, but only exacerbated these defects.

Craniofacial defects due to teratogen exposure have been shown to be mediated by their effects on neural crest cell (NCC) activity in the developing embryo. NCCs are a multipotent cell population formed after gastrulation that give rise to the majority of craniofacial tissues. NCC derivatives include facial bones, cartilage, connective tissue, teeth, neurons, glia, and vasculature. Ethanol, a well-characterized craniofacial teratogen, has been shown to alter NCC migration in zebrafish, causing facial asymmetry and increased cell death in the craniofacial region [25]. Similarly, in chickens, ethanol exposure *in ovo* induced cranial NCC death in patterns consistent with craniofacial defects observed after birth [26]. Cigarette smoke, a known craniofacial teratogen that increases the risk of cleft lip and palate, was shown to alter NCC migration *in vitro* by interaction with the aryl hydrocarbon receptor [4]. Since successful NCC proliferation, migration, and differentiation *in vivo* are critical to the normal formation of craniofacial tissues, it can be inferred that compounds altering NCC behavior *in vitro* may be craniofacially teratogenic.

The aim of this study was to determine the effects of exposure to e-cigarette aerosol mixtures (e-cigAMs) on proliferation, migration, and differentiation of murine NCCs *in vitro* and on craniofacial abnormalities of developing mouse (mammalian) embryos *in vivo*. Murine NCCs were exposed to research-grade unflavored e-cigarette aerosol mixtures (e-cigAM), made by bubbling aerosol through cold PBS. *In vivo*, murine embryos were exposed to e-cigAM throughout gestation via osmotic pump, harvested at a gestational age of 17.5d, and imaged using micro-computed tomography (microCT). A landmark-based analysis system was used to quantify differences in craniofacial morphometry from e-cigAM exposure.

Materials and Methods

E-CigAM Preparation

Electronic cigarette aerosol mixtures (e-cigAM) was created by implementing a novel method of extracting e-cigarette compounds into 1 mL of PBS for cell studies (Figure 5). A 0.16-ohm atomizer (Aspire Cleito 120 Tank, 4 mL tank) and a 150W mod (Aspire Archon 150W Mod) was used to create the various aerosols. E-cigAMs were generated using unflavored e-liquids (Table 1). The topography used to create the e-cigAMs consisted of one “vaping session” which consisted of a series of 20 3.5-second puffs (40 mL) with 30 second intervals between each puff. The solutions were then diluted (1:1000) in cell culture media to achieve desired experimental procedures. All e-cigAMs created were aliquoted and stored at -80 Celsius until needed.

Neural Crest Cell Culture

Murine cranial neural crest cells (NCCs) were seeded on human embryonic stem cell qualified reduced growth factor basement membrane matrix. They were cultured in

complete embryonic stem cell medium. The cells were cultured to confluency and plated onto Geltrex coated 24 well plates. The seeding density was 20,000 cells/cm^2. E-cigAM was diluted 1:100, 1:1000, 1:10000 in culture media and refreshed every 24 hours. For gene expression analysis, NCCs were cultured in four different media to examine angiogenesis, chondrogenesis, osteogenesis, and smooth muscle differentiation. For the angiogenesis and control groups, NCCs were cultured in embryonic stem cell complete media (ESCM); chondrogenic media was used for cells in chondrogenesis, osteogenic media was used for cells in osteogenesis. Smooth muscle differentiation was examined by NCCs being cultured in ESCM with 10% transforming growth factor beta (TGFB).

AlamarBlue Assay

AlamarBlue assay was performed to assess the cell metabolism and viability for 72 hours. After each measurement (every 24 hours), fresh medium was added to each well along with the diluted e-cigAM treatments. For each time point, 100 uL of AlamarBlue reagent was added to each well and incubated at 37 degrees Celsius for 4 hours. After the incubation period, 100 uL of media was removed and read on a plate reader at a fluorescence intensity of 560 nm.

qRT-PCR Gene Expression

Quantitative RT-PCR was performed to assess specific mRNA levels. RNA was first extracted from murine neural crest cells after 7 and 14 days using TRIzol following the manufacturer's directions. The production of cDNA was followed and real-time qPCR was performed using several primers combined with PowerUp SYBR Green Master Mix. Levels of mRNA were analyzed using a StepOnePlus real-Time PCR system for vascular endothelial growth factor A (*Vegfa*), fibroblast growth factor 2 (*Fgf2*), SOX-9, collagen-

type II-alpha-1 (*Col2a1*), runt-related transcription factor 2 (*Runx2*), osteocalcin (*Bglap*), osterix (*Sp7*), actin (*Acta2*), and glyceraldehyde 3-phosphate dehydrogenase (*Gapdh*). CT values were normalized to *Gapdh* cycle values (∆ Ct) and again to the control cycle (∆∆ Ct) values to create the fold regulation values ($2^{-\Delta\Delta Ct}$). A fold regulation change of two was determined to be significant based on $P < 0.05$ after normalization of values.

Proliferation and Cell Cycle Analysis

NCCs were grown overnight on a geltrex-coated 24-well plate in CM supplemented with e-cigAM. Cells were then incubated in media supplemented with bromodeoxyuridine (BrdU) conjugated to Alexa Fluor 647 and e-cigAM for 1.5h. Following incubation with BrdU, cells were washed, fixed, and stained with 4',6-Diamidino-2-Phenylindole (DAPI) for live cell staining. The materials were provided or made as directed in the Phase-Flow™ Alexa Fluor 647 BrdU Kit (BioLegend). Cells were then analyzed for BrdU and DAPI content with a BD LSRFortessa-X20 flow cytometer at the VCU Flow Cytometry Shared Resource Core. Flow cytometry data were analyzed using FCS Express 5.

Animal Model

Animal models were carried out in accordance with a protocol approved by the Virginia Commonwealth University Institutional Animal Care and Use Committee (VCU IACUC). E-cigAMs were aliquoted (200 µL) into commercially available osmotic pumps (ALZET, California). The release rate for all e-cigAMs were 0.25 uL/hour and the duration was 28 days. Filled pumps were implanted subcutaneously dorsally in 10 week old female C57BL/6J mice. Female mice were mated 1 week after implantation and embryos extracted at E17.5.

Micro-CT Acquisition and Analysis

Embryos (n=10/treatment) were fixed in formalin and imaged by high resolution micro-CT (Skyscan 1173 Bruker) at 60kV voltage and 133uA current at a resolution of 11.1µm. Scans were binned at 2400x2400 pixels and reconstructed using an average threshold of 55. A total of 516 landmarks and semi-landmarks were superimposed on the 3D renderings (Stratovan Checkpoint) for analysis. Twenty essential landmarks (LM) were used to assess cranial vault features and orofacial features. The cranial vault bony features were marked by LM 1 – 8. LM 9 – 18 marked the orofacial bony features.

Statistical Analysis

Essential LMs and qPCR statistical analyses were performed using GraphPad V5 software. Comparisons between groups were analyzed using ANOVA and Student's t-test where appropriate using the Tukey HSD modification and determined significance based on a p-value < 0.05. Raw landmarks coordinates were analyzed using MorphoJ software via Generalized Procrustes Analysis (GPA). Statistical relationships between groups were analyzed by canonical variate analysis (CVA) and discriminant function analysis (DFA). These relationships were shown on Principle Component Analysis (PCA) plots and bivariate plots.

Results

Morphological changes in craniofacial development show aplasia of the eye and mandible in RG 15:85 treated group and absence of eye and mandible in Almond Butter flavored group

Light microscope images of the embryonic mouse heads (lateral views) at stage 17.5 embryonic day were assessed for any overall morphological changes from the treated e-cigAM groups. Gross examination of embryonic samples revealed changes in structure

and development of the craniofacial region. E-cigAM-exposed embryos displayed shortening of the snout area with increasing VG dose (Figure 6a-d). Furthermore, in 15:85 with nicotine, aplasia of the eye and mandible were seen. While the 70:30 3D model was not significantly different compared to the control, both 30:70 and 15:85 groups, displayed a decrease in bone volume compared to the control. 15:85 displayed decreased surface areas in the nasal, frontal, parietal, and mandibular bones compared to control and all other treated groups. Transformation grids and wireframes depicted differences in shape between exposed groups and control (Figure 6e-g). Red outlines represent control group, while blue outlines represent the indicated e-cigAM treated group. While 70:30 and 30:70 groups did not show a significant difference, 15:85 showed differences in the frontal/parietal bone structure compared to the control. Light microscopic images of embryos exposed to flavored e-cigAM were displayed in Figure 7. Almond Butter (Figure 7b) showed a major craniofacial abnormality with the absence of the mandible and the eye. Pineapple and Coconut (Figure 7c) and Strawberry Shortcake (Figure 7d) also showed smaller bone surface area in the nasal and mandibular regions Overall, analysis suggests that there are small shape changes that are VG dose-dependent.

Absolute changes in vault and orofacial landmark measurements show statistically different shape changes

Twenty essential landmarks (LMs) were used to assess craniofacial geometry. These specific landmarks were chosen for analysis due to their representation of morphological traits of the skull and craniofacial structures during late pre-natal life (17.5 days post-conception) in mice [22]. LMs located on the cranial vault were marked by LM 1 – 8 (Table 2) which consisted of the frontal bone, parietal bone, lacrimal bone, maxilla, and

occipital bone. LM 8 – 18 marked orofacial bony sites which consisted of the palatine foramen, premaxilla, malar process, zygoma, and mandible (Table 3). Landmark placement on 3D models for measurement assessments were displayed on Figure 8 while landmark measurements were displayed in Figure 9 (unflavored e-cigAM) and Figure 10 (flavored e-cigAM). .

Embryos exposed to unflavored e-cigAM showed a PG:VG dependence in cranial and orofacial landmark measurements (Figure 9). The height of the nasal bone (LM 4) was significantly reduced in all three e-cigAM groups compared to the control embryos. 15:85 showed the most prominent reduction (44.5%) compared to the control and a 40% reduction compared to the two other PG:VG ratio e-cigAMs. Accordingly, the width of the posterior cranium (LM 5) was significantly different in all e-cigAM exposed groups compared to the control. The distance measurement in 70:30 decreased 15.8%; whereas both 30:70 (20.8%) and 15:85 (29.6%) increased compared to the control. The latter group showed a substantial increase compared to all other groups. The overall width (LM 1) and length (LM 2) of the cranial region in 15:85 e-cigAM-exposed embryos were significantly reduced by 16.7% and 17.2% respectively related to the control. The height of the cranial region (LM 3) of treated e-cigAM groups of 30:70 and 15:85 were both reduced by 17.6% and 32.3% respectively compared to the control. Additionally, the 15:85 group was significantly reduced (14.8%) compared to the 30:70 group. The length of the superior aspect of the cranium from all three treated groups (70:30 (11.5%), 30:70 (15.4%), and 15:85 (19.2%)) were significantly reduced in a linear fashion in relation to the control group. These data again suggest that overall shape changes were VG dose-dependent, with 15:85 showing the most shape changes in the cranial region (Figure 9a).

Most of the treated groups in the orofacial landmark features were significantly different compared to the respective control (Figure 9b). In both the left (LM 9) and right (LM 10) palatine foramen, only 70:30 resulted in a significant reduction of 12.5%. Groups 70:30 and 30:70 were statistically different from the control in the left (LM 11) (19.9%, 14.3%) and right (LM 12) (24.9%, 14.9%) pre-maxilla, right (LM 13) (42.9%, 23.8%) and left (LM 15) (20.0%, 25.0%) zygoma, right (LM 14) (18.2%) and left (LM 16) (26.1%) malar process, and right (LM 17) (9.7%, 9.6%) and left (LM 18) (12.9%, 11.3%) mandible, respectively. The right and left zygoma (52.4%, 55.0%), right and left malar process (45.5%, 39.1%), and right and left mandible (36.7%, 37.1%) in 15:85 was significantly shorter than control. Overall, the inhibitory effects of VG concentration were preserved, with 15:85 e-cigAM-exposed mice exhibiting the greatest changes in craniofacial bone structure.

Cranial and orofacial landmark measurements in embryos exposed to flavored e-cigAM were displayed in Figure 10. Pineapple & Coconut and/or Strawberry Shortcake were significantly different in all but one cranial vault LMs. Pineapple & Coconut decreased significantly by 12.5% in the overall width (LM 1) and by 13.89% in the overall length (LM 2) of the cranium compared to the control. The height of the cranial region (LM 3) in all three flavored e-cigAM (Almond Butter, Pineapple Coconut, and Strawberry Shortcake) was significantly reduced (13.43%, 36.36%, and 27.27%) compared to the control. The height between the nasal bone and the anteroinferior point of the mandible (LM 4) in Pineapple & Coconut was significantly reduced (41.33%) compared to the control. Additionally, the width of the posterior cranium (LM 5) was significantly increased in all three flavored groups (Almond Butter (14.29%), Pineapple & Coconut (35.14%),

Strawberry Shortcake (25.00%)) compared to the control. Overall, we can suggest that even more than PG – VG ratio dependence, the addition of flavorings and nicotine also has an effect on cranial fault features (Figure 10a).

Flavored e-cigAMs and their orofacial features were compared in Figure 10b. In both the left (LM 9) and right (LM 10) palatine foramen, only Almond Butter had a significant reduction of 22.58% compared to the control. All three flavored e-cigAMs displayed a significant difference in landmark measurements in the both the left and right of the zygoma, malar process, and the mandible. Almond Butter resulted in an average of 21.67% reduction in all three landmarks compared to the control. Strawberry Shortcake revealed an average of 28.16% decrease, whereas Pineapple & Coconut showed the greatest average decrease at 36.86% in all three landmark measurements compared to the control. Again these data shows that flavorings and nicotine have an exacerbated effect on all LMs.

Quantitative analysis show significant differences in Procrustes distances of 70:30 and 15:85 PG:VG groups and all flavored groups compared to control

To normalize shape change in craniofacial bones following e-cigAM exposure, geometric morphometry (GM) techniques were utilized. GM methods consists of a multivariate analysis that is performed by acquiring landmarks and semi-landmarks and implementing an ordination technique called Procrustes superimposition in order to perform principal component analysis (PCA), and discriminate function analysis (DFA). Procrustes superimposition analyzes objects to minimize the differences between landmark configurations by translating, rotating, and scaling them to obtain shape coordinates and Procrustes distances. PCA was performed to illustrate shape changes

within samples and ultimately groups. PCA takes into account the large number of LM-based patterns of shape change in samples and make them easier to interpret by replacing the original variables with principal components (account for a portion of total variance) that are linear combinations of the original variables and independent of each other [11]. The first two principal components produced from the LM data displayed over 50% of the variance within all groups. All groups were significantly different from each other in both PC1 and PC2, with PC2 being the most distinct. Clustering of the individuals signifies little variance within each other, while individuals in groups that were more widely dispersed indicated a high degree of variance within the group. This can be seen in the 30:70 group (Figure 11a).

DFA was performed to illustrate shape changes between groups, specifically a treated group (70:30, 30:70, or 15:85) and flavored groups (Figure 12c-e) versus control. The results of the DFA showed that 30:70's shape change was not statistically significant from the control group (Procrustes distance: 0.19589295, p-value: 0.3949) (Figure 11c). However, groups 70:30 (Procrustes distance: 0.17050213, p-value: <0.001) and 15:85 (Procrustes distance: 0.17929203, p-value: <0.001) were (Figure 11b, d). All flavored groups (Almond Butter (Procrustes distance: 0.16371728, p-value: <0.001), Pineapple and Coconut (Procrustes distance: 0.20874694), p-value: <0.001), Strawberry Shortcake (Procrustes distance: 0.16221867, p-value: <0.001) showed a significant difference in Procrustes distance compared to the control. The most prominent areas affected by exposure were the nasal/snout region and the mandible.

Qualitative analysis of blood vessels in unflavored and flavored e-cigAM show possible underdevelopment of blood vessel formation

Murine embryos were stained with iodine for two weeks following an established protocol [27]. Afterwards, embryos were scanned using a μCT scanner and 3D models were created. Maximum intensity projection (MIP) imagers of the vasculature in the cranial region are shown of unflavored and flavored groups in Figure 13. Views from the superior, anterior, and lateral views show the major cerebral arteries such as the inner cerebral artery (ICA) and basilar artery (BA) in most of the treated groups. Difference in MIP colored images represents a different treated groups. Further analysis of the vasculature was performed using a micro-CT analysis software.

Quantitative μ-CT analysis of angiogenesis showed a PG – VG ratio dependence in most vascular parameters that were measured

Morphometric analysis of the craniofacial vascular network was also performed by iodine staining mouse embryos and micro-CT scanning. The parameters that were analyzed included vascular volume, connectivity, thickness, thickness distribution, vessel number, separation, and degree of anisotropy. Vessel thickness distribution was defined as the local thickness at each voxel in the region of interest (ROI) as the diameter of the largest sphere that contains both the voxel and within the ROI. Vessel thickness was normally distributed in the control group (Figure 14a), while 70:30 had a higher percentage of smaller vessel thickness ranging between 0.005 < 0.050 mm (Figure 14b). Strawberry Shortcake had the next highest percentage of small vessel thickness ranging from 0.051 - <0.100 mm (Figure 14e). 15:85 had the highest vessel thickness at <300 mm (Figure 14d). Average vessel thickness (Figure 15c) was VG-dependent, with 70:30

having the smallest thickness and 15:85 having the largest vessel thickness. PG – VG ratio was preserved in vascular volume (Figure 15a) where 15:85 was significantly reduced compared to all other groups. The addition of flavoring further reduced the volume. Connectivity is defined as the maximum number of vessels that can be cut without separating the structure. Connectivity also relates directly to the strength of the structure. As the VG ratio increases, the connectivity of the each groups is reduced, with all four groups showing significant difference compared to the control group (Figure 15b). The strongest effect is seen in the flavored group. Anisotropy describes the orientation of the 3D vascular bed, where 1.0 suggests a perfectly isotropic structure. A higher degree of anisotropy indicates a vascular bed with optimal material direction. Strawberry Shortcake and 15:85 had the highest degree of anisotropy compared to all other groups analyzed (Figure 15f).

E-cigAM exposure reduces neural crest cell viability

NCC viability was assessed after exposure to e-cigAMs produced from varying ratios of PG:VG ± nicotine (Table 1). All e-cigAMs attenuated metabolic activity compared to complete stem cell media and PBS exposure controls, and nicotine enhanced this effect (Figure 16). Overall, NCC viability decreased in a nicotine and VG dose-dependent fashion.

E-cigAM exposure attenuates expression of genetic markers of NCC differentiation

To determine the effect of e-cigAM on NCC differentiation, cells were exposed to e-cigAMs while growing in angiogenic, chondrogenic, osteogenic, or smooth muscle induction media. Angiogenic markers *Vegf* and *Fgf2* were not as highly upregulated compared to control groups (Figure 17a). Expression of *Vegf* and *Fgf2* markers were

significantly lower in both 70:30+ nicotine (7030+) and 30:70+ nicotine (30:70+) compared to their respective no-nicotine (70:30-, 30:70-) and control counterparts. Markers of differentiation in 15:85 ± nicotine (15:85±) groups were not as highly upregulated in NCCs compared to the control group, and there were no differences in gene upregulation with or without nicotine in these groups with respect to *Vegf* and *Fgf2*. This may be because the nicotine concentration in 15:85 e-cigAMs is much lower than in 70:30 or 30:70 e-liquids due to decreased nicotine solubility in high-VG preparations.

Chondrogenic marker upregulation in induction media was also affected by e-cigAM exposure (Figure 17b). *Sox9* and *Col2a1* upregulation was significantly attenuated in all e-cigAM groups, with nicotine potentiating this change. Similarly to angiogenic markers, the differences between 15:85+ and 15:85- were smaller or insignificant compared to other ± nicotine groups, suggesting that nicotine dose has an effect on chondrogenic differentiation of NCCs as well.

Osteoblast differentiation was assessed by gene expression of osteogenic markers *Runx2*, *Bglap* (osteocalcin), and *Sp7* (osterix). All ecig-AMs attenuated the upregulation of these markers in cells cultured in osteogenic induction media, and nicotine enhanced this effect (Figure 17c).

Smooth muscle differentiation was examined by the smooth muscle actin α2 (*Acta2*) marker. All treated groups were significantly different than the control. All no-nicotine groups (70:30-, 30:70-, 15:85-) had significantly lower *Acta2* mRNA than controls (Figure 17d). Interestingly, the presence of nicotine upregulated *Acta2* relative to no-nicotine ecig-AMs.

Ecig-AM exposure inhibits NCC migration in a VG and nicotine dose-dependent manner

The effect of e-cigAM on NCC migration was evaluated by transwell invasion assay, with e-cigAM added to both media inside and outside the insert. A decrease in migration was observed with exposure to all e-cigAM types (Figure 18a). When comparing exposure to e-cigAMs without nicotine, migratory inhibition was found to be dependent on VG dose (Figure 18b). When nicotine-only e-cigAMs were compared, VG dose-dependence was preserved, but the inhibitory effect on migration was enhanced (Figure 18c). These data suggest that e-cigAMs inhibit NCC migration in a VG and nicotine dose-dependent manner.

E-cigAM inhibits NCC proliferation and cell cycling

To evaluate the effect of e-cigAM on proliferation, NCCs were cultured in e-cigAM-supplemented media overnight, then incubated with fluorescently-tagged BrdU to measure DNA replication. Following DAPI staining for live cells, the proportion of DAPI+ cells that incorporated fluorescent BrdU was measured by flow cytometry. Exposure to e-cigAM decreased BrdU incorporation in nearly all groups, with an enhanced effect when nicotine is added (Figure 19a). Exposure to 70:30- e-cigAM produced a decrease in BrdU incorporation, although the effect was not statistically significant. Representative dot plots (flow cytometric analysis) of the effect of e-cigAM exposure on cell cycle is shown in Figure 19b-e. While not shown, the percentage of GFP+ and DAPI+ cells were >99%, indicating high cell viability of samples. Together, these data show that e-cigAMs exert a significant effect on NCC cell cycle and proliferation that appears to be partially VG and nicotine dose-dependent.

Chapter 4: Discussion and Future Directions

Discussion

Electronic cigarettes have been burgeoning in popularity since their introduction in 2004, and since then, they have evolved from simple disposable electronic nicotine delivery devices (ENDs) to larger refillable ones capable of generating aerosols from thousands of different e-liquids, each containing varying amounts of nicotine and flavor compound [2], [28]. While e-cigarettes are generally deemed safer than cigarettes, their effects on pregnancy were not fully evaluated prior to market introduction; unfortunately, this falsely-conceived notion of safety has led some women to use e-cigarettes during pregnancy [16]. Furthermore, previous work by our lab demonstrated craniofacial anomalies in the formation of cartilaginous, muscular, and vascular structures in *Xenopus laevis* embryos, as well as decreased markers of chondrogenic and angiogenic differentiation in murine NCCs, when exposed to certain e-cigAMs [24]. These findings underscored a need to more thoroughly explore the effects of e-cigarettes on embryonic development in mammalian models.

This study sought to further characterize the effects of research-grade e-cigAM on differences seen in shape morphology, specifically which tissues maybe affected and NCC differentiation, migration, and proliferation. Morphological changes in craniofacial development revealed aplasia of the eye and mandible in unflavored 15:85 treated group. This underdevelopment suggests that the neural ectoderm, the surface ectoderm, and the periocular mesenchyme, which are all responsible for the formation of the mammalian eye, may have been affected. Additionally, several studies have reported the presence/role of retinoic acid (RA) activity during the formation of the eye (optical vesicle

formation at E8.5, lens placode at E8.5, and periocular mesenchyme at E10.25) [29]–[32]. This leads to the notion that RA activity must also be analyzed in relation to e-cig aerosol exposure.

Absolute quantitative and geometric morphometric analysis showed changes in the vault and orofacial landmarks and also Procrustes distance suggesting midface hypoplasia in some of the treated groups. Mid-facial development occurs through a coordinated effort of various cellular mechanisms and processes including the frontonasal prominence, the paired lateral and medial nasal processes, and the paired maxillary processes. Changes in any of these processes as well as mutations in major signaling pathways (bone morphogenetic protein [BMP], fibroblast growth factor [FGF], Notching signaling, platelet-derived growth factor [PDGF], transforming growth factor-beta [TGFβ] and WNT signaling) have been hypothesized as contributing to the factors associated with mid-facial birth defects [33]. Additionally, environmental risk factors (such as smoking e-cigs) may drive these mutations.

Quantitative μ-CT analysis of angiogenesis showed a PG-VG ratio dependence in vascular parameters of vascular volume, vessel thickness, vessel separation, connectivity, and degree of anisotropy. While vascular volume and connectivity displayed a linearly decreasing trend in PG – VG ratio; vessel thickness, vessel separation, and degree of anisotropy exhibited a positive trend in PG – VG. These data suggest that vascular development maybe affected by various ratios of PG – VG. It is well known that craniofacial dysmorphology results from the inappropriate interactions between blood and bone cells during the development of the skeleton [34], [35]. Blood vessel formation occurs through two associated mechanisms: vasculogenesis and angiogenesis.

Specifically, the process of intramembranous ossification (angiogenesis), the main mechanism of the formation of the craniofacial bones, may be affected due to e-cig exposure of various PG – VG ratios. During embryonic development, the capillaries move into loose mesenchyme [36]. Once there mesenchymal cells secrete VEGF, which in turn attract endothelial cells. Small vessels invade near the initial ossification site where the bone associates with a network of blood vessels. This association of vascular invasion and bone ossification continues until bone expansion occurs in all directions. VEGF is the primary growth factor during angiogenesis which is commonly supplied by hypertrophic chondrocytes, mesenchymal cells and endothelial cells [37]. However, during the development of flat/cranial bones, cranial NCCs and NCC-derived cells can also be a primary source of VEGF which supports vascular growth in the developing jaw [38]. Therefore, an insufficient supply of VEGF derived from NCC derived tissues may exhibit mandibular hypoplasia [39]. This further places the importance of how e-cigs may affect the vasculature of the developing embryo which in turn can affect the developing craniofacial bone structures.

Exposure to e-cigAM inhibited production of gene markers of chondrogenic and osteogenic differentiation in NCCs. E-cigAM exposure also inhibited NCC migration in an invasion assay in a manner dependent on the dose of both VG and nicotine. NCC proliferation and cell cycling were inhibited in a manner similar to migration. Together with previous published work, these data show that e-cigAMs exert adverse effects on NCC behaviors and suggest teratogenic risk. These results support further exploration of the effects of e-cigarettes on pregnancy.

Several twin and family studies have shown that the gene-environment (GxE) interactions caused by smoking have been informative in highlighting the influence of gene changes as an association of both the measured phenotype and the environment [40]. Conversely, it is not well known how the effect on various genes on different phenotypes of cigarette use changes in relation to the environment. So far genome wide association studies (GWAS) have shown variants of nicotinic receptor genes (*CHRNA5-CHRNA3-CHRNB4)* have been associated with the number of cigarettes per day (CPD), nicotine dependence, and heavy smoking habits [41]–[45]. Additionally, the risk of chronic obstructive pulmonary disease (COPD) and lung cancer was linked to the same locus of genes in several GWAS [46]. It has been studied that the serotonin transporter gene (*5-HTTLPR*) and the dopaminergic system are also believed to play a role in nicotine addiction and dependence [47]. Just as genes play a role in the cigarette, social and environmental factors such as sociodemographic characteristics, family cigarette use, and peer cigarette use also contribute to the use of tobacco smoking. It is important to translate these methodologies to study if there are similar findings in genes and environment that pertain to e-cig use characteristics as well.

Overall, this paper produced similar results compared to our previously published literature on the effects of e-cigAM on *Xenopus laevis* embryos. Though the defects mentioned in this paper were not as prominent compared to the clefting and mid-face hypoplasia found in the *Xenopus laevis*, it is important to note the translation of abnormalities from an amphibian animal model to a mammalian animal model.

Significant limitations exist in the study of e-cigarettes. Due to the vast number of combinations of e-liquid, devices, and heating power, as well as varied manufacturing

practices, it is impossible to formulate a comprehensive study of all commercially-available products. Studies attempting to identify the compounds in e-cigarette aerosol have found varying levels of aldehydes, volatile aromatic compounds, polycyclic aromatic hydrocarbons, heavy metals, and nicotine, all depending on the aforementioned variables [12]. Each of these compounds can exert pharmacologic and toxic effects on cells and may have contributed to the observed behaviors of the NCCs in this study [23], [25], [26], [48]. For example, the VG-dependent effects of e-cigAM may be due to increased production of acrolein, a known toxicant, and product of VG heating [20],[49]. Further characterization of the compounds produced by e-cigarettes, as well as those found in the e-cigAM model of exposure, will enhance our understanding of the physiologic effects of these products. Additionally, this study focused solely on C57BL/6J mice, but it is necessary to also study various breeds that are susceptible to craniofacial abnormalities to see if the use of e-cigs increase these defects.

Future Directions

Future studies include exploring the effects of e-cigarette exposure on craniofacial development *in vivo* further. Identifying which compounds cross the fetal-placental barrier, to what extent they cross, and how they affect NCCs in the embryo will strengthen the proposed link between e-cigarettes and craniofacial teratogenicity. Additionally, the role of flavor compounds in modulating the effects of e-cigarettes should be explored, both *in vitro* and *in vivo* in a mammalian model. The effects of second- and third-hand exposure should also be explored in these models. Our study is the first to show that exposure to e-cig aerosol may cause some craniofacial abnormalities in a mammalian mouse model. Additionally, e-cigAMs adversely affect murine NCC differentiation, migration, and

proliferation in vitro, suggesting potential teratogenicity of e-cigarettes when used by pregnant mothers. Further study of e-cigarettes' effect on pregnancy is important as the use of these products becomes more ubiquitous.

References

[1] United States Department of Health and Human Services, “The Health Consequences of Smoking—50 Years of Progress A Report of the Surgeon General,” *A Rep. Surg. Gen.*, p. 1081, 2014.

[2] A. Breland, E. Soule, A. Lopez, C. Ramôa, A. El-Hellani, and T. Eissenberg, “Electronic cigarettes: what are they and what do they do?,” *Annals of the New York Academy of Sciences*, vol. 1394, no. 1. pp. 5–30, 2017.

[3] A. Jamal *et al.*, “Tobacco Use Among Middle and High School Students — United States, 2011–2016,” *MMWR. Morb. Mortal. Wkly. Rep.*, vol. 66, no. 23, pp. 597–603, 2017.

[4] A. Sanbe *et al.*, “Inhibitory effects of cigarette smoke extract on neural crest migration occur through suppression of R-spondin1 expression via aryl hydrocarbon receptor,” *Naunyn. Schmiedebergs. Arch. Pharmacol.*, vol. 380, no. 6, pp. 569–576, 2009.

[5] U.S. Surgeon General, “Preventing Tobacco Use Among Youth and Young Adults. A report from the Surgeon General,” *U.S. Dep. Heal. Hum. Serv.*, p. 1395, 2012.

[6] C. Schoenborn and R. Gindi, “Electronic cigarette use among adults: United States, 2014,” *Natl. Cent. Heal. Stat.*, no. 217, pp. 1–7, 2015.

[7] D. R. Cordero, S. Brugmann, Y. Chu, R. Bajpai, M. Jame, and J. A. Helms, “Cranial neural crest cells on the move: Their roles in craniofacial development,” *Am. J. Med. Genet. Part A*, vol. 155, no. 2, pp. 270–279, 2011.

[8] T. N. Snider and Y. Mishina, “Cranial neural crest cell contribution to craniofacial

formation, pathology, and future directions in tissue engineering," *Birth Defects Res. Part C - Embryo Today Rev.*, vol. 102, no. 3, pp. 324–332, 2014.

[9] P. A. Trainor, "Craniofacial birth defects: The role of neural crest cells in the etiology and pathogenesis of Treacher Collins syndrome and the potential for prevention," *American Journal of Medical Genetics, Part A*, vol. 152 A, no. 12. pp. 2984–2994, 2010.

[10] T. P. Hill, "Institute of Mathematical Statistics is collaborating with JSTOR to digitize, preserve, and extend access to Statistical Science. ® www.jstor.org," *Stat. Sci.*, vol. 10, no. 4, pp. 354–363, 1995.

[11] M. Zelditch, D. Swiderski, and H. D. Sheets, *Geometric Morphometrics for Biologists*, 2nd ed. San Diego: Elsevier, 2012.

[12] T. Cheng, "Chemical evaluation of electronic cigarettes," *Tob. Control*, vol. 23, no. SUPPL. 2, 2014.

[13] E. National Academies of Sciences and Medicine *et al.*, "Public Health Consequences of E-Cigarettes," *JAMA Intern. Med.*, pp. 1–613, 2018.

[14] C. A. Hess, P. Olmedo, A. Navas-Acien, W. Goessler, J. E. Cohen, and A. M. Rule, "E-cigarettes as a source of toxic and potentially carcinogenic metals," *Environ. Res.*, 2017.

[15] P. Olmedo *et al.*, "Metal Concentrations in e-Cigarette Liquid and Aerosol Samples: The Contribution of Metallic Coils," *Environmental Health Perspectives*, 2018. .

[16] S. Baeza-Loya *et al.*, "Perceptions about e-cigarette safety may lead to e-smoking during pregnancy," *Bull. Menninger Clin.*, vol. 78, no. 3, pp. 243–252, 2014.

[17] A. McCubbin, A. Fallin-Bennett, J. Barnett, and K. Ashford, “Perceptions and use of electronic cigarettes in pregnancy,” *Health Education Research*, vol. 32, no. 1. pp. 22–32, 2017.

[18] D. Nicoletti, L. D. Appel, P. Siedersberger Neto, G. W. Guimarães, and L. Zhang, “Maternal smoking during pregnancy and birth defects in children: a systematic review with meta-analysis.,” *Cad. saúde pública*, vol. 30, no. 12, pp. 2491–529, 2014.

[19] C. V Ananth, J. C. Smulian, and A. M. Vintzileos, “Incidence of placental abruption in relation to cigarette smoking and hypertensive disorders during pregnancy: A meta-analysis of observational studies,” *Obstet. Gynecol.*, vol. 93, no. 4 SUPPL., pp. 622–628, 1999.

[20] R. Ion and A. L. Bernal, “Smoking and preterm birth,” *Reproductive Sciences*, vol. 22, no. 8. pp. 918–926, 2015.

[21] X. Lu *et al.*, “Characterization of complex hydrocarbons in cigarette smoke condensate by gas chromatography-mass spectrometry and comprehensive two-dimensional gas chromatography-time-of-flight mass spectrometry,” *J. Chromatogr. A*, vol. 1043, no. 2, pp. 265–273, 2004.

[22] J. Barbeito-Andrés, P. Gonzalez, and B. Hallgrímsson, “Prenatal development of skull and brain in a mouse model of growth restriction,” *Rev. Argentina Antropol. Biológica*, vol. 18, no. 1, pp. 1–13, 2016.

[23] F. Ozturk, E. Sheldon, J. Sharma, K. M. Canturk, H. H. Otu, and A. Nawshad, “Nicotine exposure during pregnancy results in persistent midline epithelial seam with improper palatal fusion,” *Nicotine Tob. Res.*, vol. 18, no. 5, pp. 604–612,

2016.

[24] A. E. Kennedy, S. Kandalam, R. Olivares-Navarrete, and A. J. G. Dickinson, “E-cigarette aerosol exposure can cause craniofacial defects in Xenopus laevis embryos and mammalian neural crest cells,” *PLoS One*, vol. 12, no. 9, p. e0185729, 2017.

[25] A. Massarsky, A. Abdel, L. Glazer, E. D. Levin, and R. T. Di Giulio, “Exposure to 1,2-Propanediol Impacts Early Development of Zebrafish (Danio rerio) and Induces Hyperactivity.,” *Zebrafish*, vol. 14, no. 3, pp. 216–222, 2017.

[26] M. M. Cartwright and S. M. Smith, “Increased Cell Death and Reduced Neural Crest Cell Numbers in Ethanol-Exposed Embryos: Partial Basis for the Fetal Alcohol Syndrome Phenotype,” *Alcohol. Clin. Exp. Res.*, vol. 19, no. 2, pp. 378–386, 1995.

[27] K. Degenhardt, A. C. Wright, D. Horng, A. Padmanabhan, and J. A. Epstein, “Rapid 3D phenotyping of cardiovascular development in mouse embryos by micro-CT with iodine staining,” *Circ. Cardiovasc. Imaging*, 2010.

[28] A. M. Glasser *et al.*, “Overview of Electronic Nicotine Delivery Systems: A Systematic Review,” *American Journal of Preventive Medicine*, vol. 52, no. 2. pp. e33–e66, 2017.

[29] W. Heavner and L. Pevny, “Eye development and retinogenesis,” *Cold Spring Harb. Perspect. Biol.*, 2012.

[30] A. Cvekl and W.-L. Wang, “Retinoic acid signaling in mammalian eye development,” *Exp. Eye Res.*, 2009.

[31] F. A. Mic, A. Molotkov, N. Molotkova, and G. Duester, “Raldh2 expression in optic

vesicle generates a retinoic acid signal needed for invagination of retina during optic cup formation," *Dev. Dyn.*, 2004.

[32] A. Molotkov, "Retinoic acid guides eye morphogenetic movements via paracrine signaling but is unnecessary for retinal dorsoventral patterning," *Development*, 2006.

[33] A. Suzuki, D. R. Sangani, A. Ansari, and J. Iwata, "Molecular mechanisms of midfacial developmental defects," *Developmental Dynamics*. 2016.

[34] C. J. Percival and J. T. Richtsmeier, "Angiogenesis and intramembranous osteogenesis," *Developmental Dynamics*. 2013.

[35] C. J. Percival and C. J. Percival, "The influence of angiogenesis on craniofacial development and evolution by," *Penn State*, vol. PhD. Thesi, no. May, 2013.

[36] T. J. Thompson, P. D. Owens, and D. J. Wilson, "Intramembranous osteogenesis and angiogenesis in the chick embryo.," *J. Anat.*, 1989.

[37] G. Breier, U. Albrecht, S. Sterrer, and W. Risau, "Expression of vascular endothelial growth factor during embryonic angiogenesis and endothelial cell differentiation," *Development*, vol. 114, pp. 521–532, 1992.

[38] S. Wiszniak, F. E. Mackenzie, P. Anderson, S. Kabbara, C. Ruhrberg, and Q. Schwarz, "Neural crest cell-derived VEGF promotes embryonic jaw extension," *Proc. Natl. Acad. Sci.*, 2015.

[39] J. Filipowska, K. A. Tomaszewski, Ł. Niedźwiedzki, J. A. Walocha, and T. Niedźwiedzki, "The role of vasculature in bone development, regeneration and proper systemic functioning," *Angiogenesis*. 2017.

[40] R. J. Rose, U. Broms, T. Korhonen, D. . Dick, and J. Kaprio, "Genetics of

Smoking Behavior," in *Handbook of Behavior Genetics*, New York, New York, USA: Kim YK, 2009, pp. 411–432.

[41] X. Chen *et al.*, "Variants in nicotinic acetylcholine receptors alpha5 and alpha3 increase risks to nicotine dependence.," *Am. J. Med. Genet. B. Neuropsychiatr. Genet.*, 2009.

[42] S. F. Saccone *et al.*, "Cholinergic nicotinic receptor genes implicated in a nicotine dependence association study targeting 348 candidate genes with 3713 SNPs," *Hum. Mol. Genet.*, 2007.

[43] L. E. Hong *et al.*, "A CHRNA5 allele related to nicotine addiction and schizophrenia," *Genes, Brain Behav.*, 2011.

[44] V. L. Stevens *et al.*, "Nicotinic receptor gene variants influence susceptibility to heavy smoking.," *Cancer Epidemiol. Biomarkers Prev.*, 2008.

[45] M. S. Conlon and M. A. Bewick, "Single nucleotide polymorphisms in CHRNA5 rs16969968, CHRNA3 rs578776, and LOC123688 rs8034191 are associated with heaviness of smoking in women in Northeastern Ontario, Canada.," *Nicotine Tob. Res.*, vol. 13, no. 11, pp. 1076–1083, 2011.

[46] S. M. Hartz *et al.*, "Increased genetic vulnerability to smoking at CHRNA5 in early-onset smokers," *Arch. Gen. Psychiatry*, 2012.

[47] E. Do and H. Maes, "Narrative review of genes, environment, and cigarettes," *Annals of Medicine*, vol. 48, no. 5. pp. 337–351, 2016.

[48] R. Da Lee *et al.*, "Neurotoxic Effects of Alcohol and Acetaldehyde During Embryonic Development," *J. Toxicol. Environ. Heal. Part A*, vol. 68, no. 23–24, pp. 2147–2162, 2005.

[49] J. F. Stevens and C. S. Maier, “Acrolein: Sources, metabolism, and biomolecular interactions relevant to human health and disease,” *Molecular Nutrition and Food Research*, vol. 52, no. 1. pp. 7–25, 2008.

List of Figures

Figure 1: Various e-cigarette products. E-cigs have rapidly diversified ranging from first generation e-cigarettes such as ‘cigalikes’ to third generation e-cigarettes such as ‘e-cig tanks and mods’. All e-cigarettes are accompanied with e-liquids.

Figure 2: Components of e-cigarettes. E-cigs have rapidly diversified ranging from first generation e-cigarettes such as ‘cigalikes’ to third generation e-cigarettes such as ‘e-cig tanks and mods’. All e-cigarettes are accompanied with e-liquids, atomizers, reservoirs, and a mouthpiece.

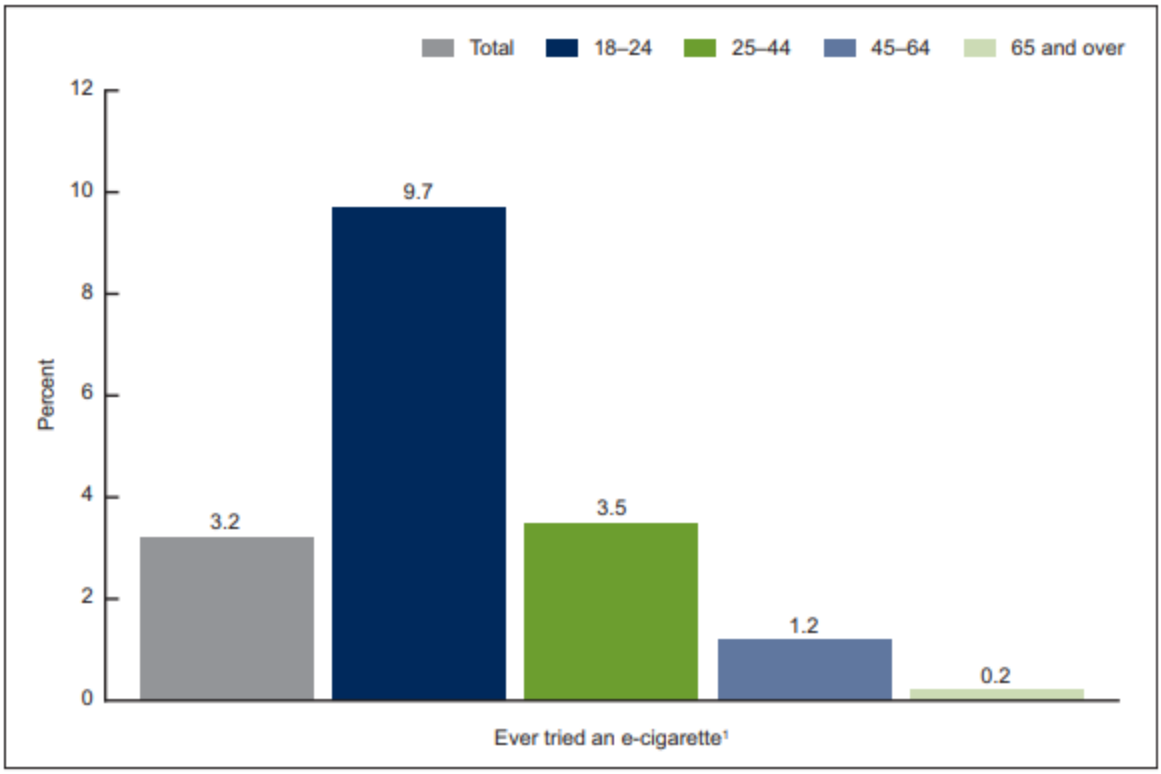

Figure 3: Percentage of Never Cigarettes Smokers Who Ever Tried an E-Cigarette. Among the adults who were surveyed, 17.8% had never smoked a cigarette, tried an e-cigarette at least once. Among these 17.8% percent of never cigarette smokers, young adults between 18-24 were more likely than older adults to have tried e-cigarettes.

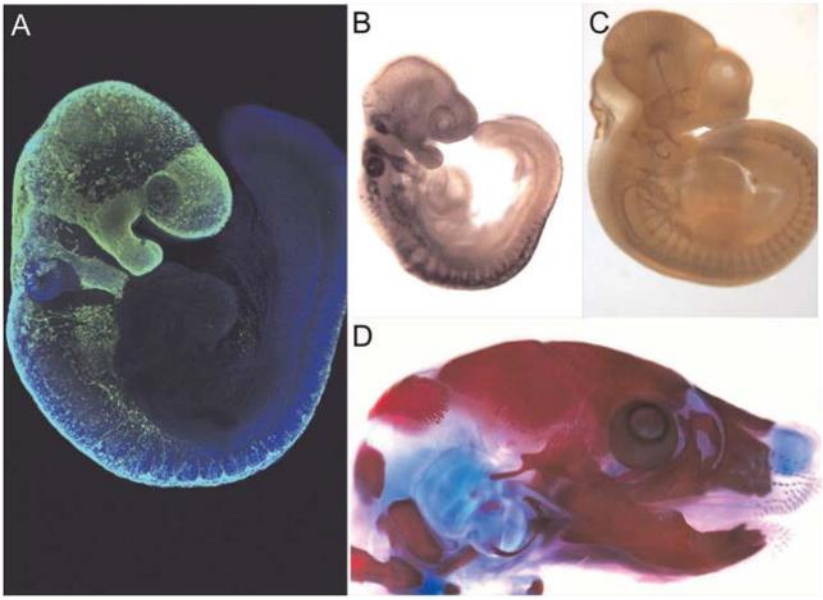

Figure 4: Neural Crest Cell (NCC) Migration and Differentiation. (A) Embryonic day 9.5 mouse embryo showing migrating neural crest cells stained with green fluorescent protein (GFP). **(B-C)** Sox10 (B) and neurofilament immunostaining (C) of E9.5 and E10.5 day mouse embryo. **(D)** Alizirin red (bone) and alcian blue (cartilage) staining of E18.5 day mouse embryo.

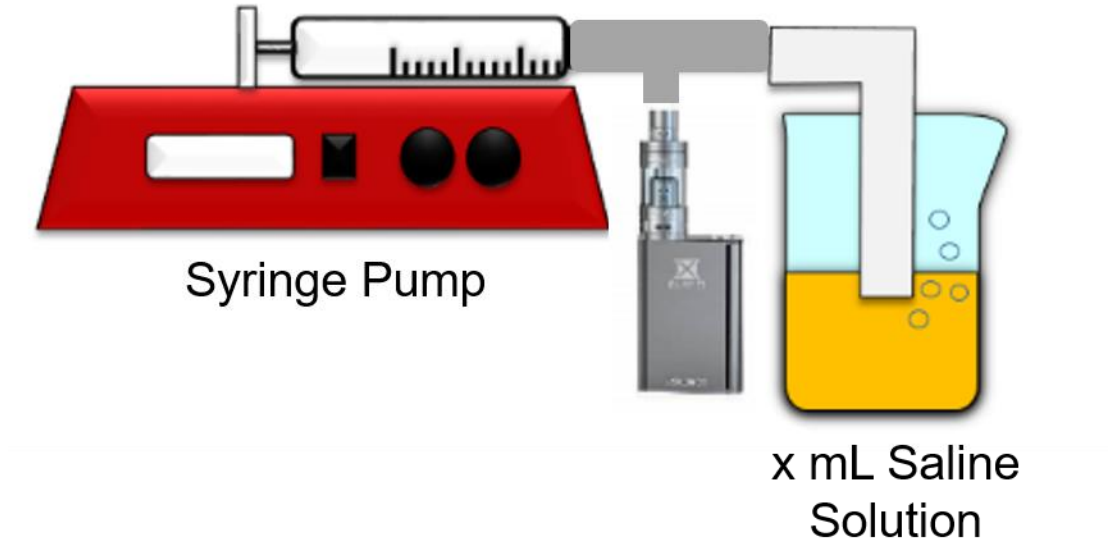

Figure 5: Schematic of implementation of a novel method. Syringe is used to extract electronic cigarette smoke. The smoke is condensed into phosphate buffered solution (PBS).

Table 1. The e-liquids tested on neural crest cell studies.

The manufacturer, nicotine concentration in mg/mL, propylene glycol to vegetable glycerin ratio are as reported on the e-liquid packaging.

Name	Manufacturer	Nicotine Concentration	PG	VG
Unflavored (RG) 70:30	AVAIL	0 mg/mL	70	30
Unflavored (RG) 70:30	AVAIL	2.4 mg/mL	70	30
Unflavored (RG) 30:70	AVAIL	0 mg/mL	30	70
Unflavored (RG) 30:70	AVAIL	2.4 mg/mL	30	70
Unflavored (RG) 15:85	AVAIL	0 mg/mL	15	85
Unflavored (RG) 15:85	AVAIL	0.6 mg/mL	15	85

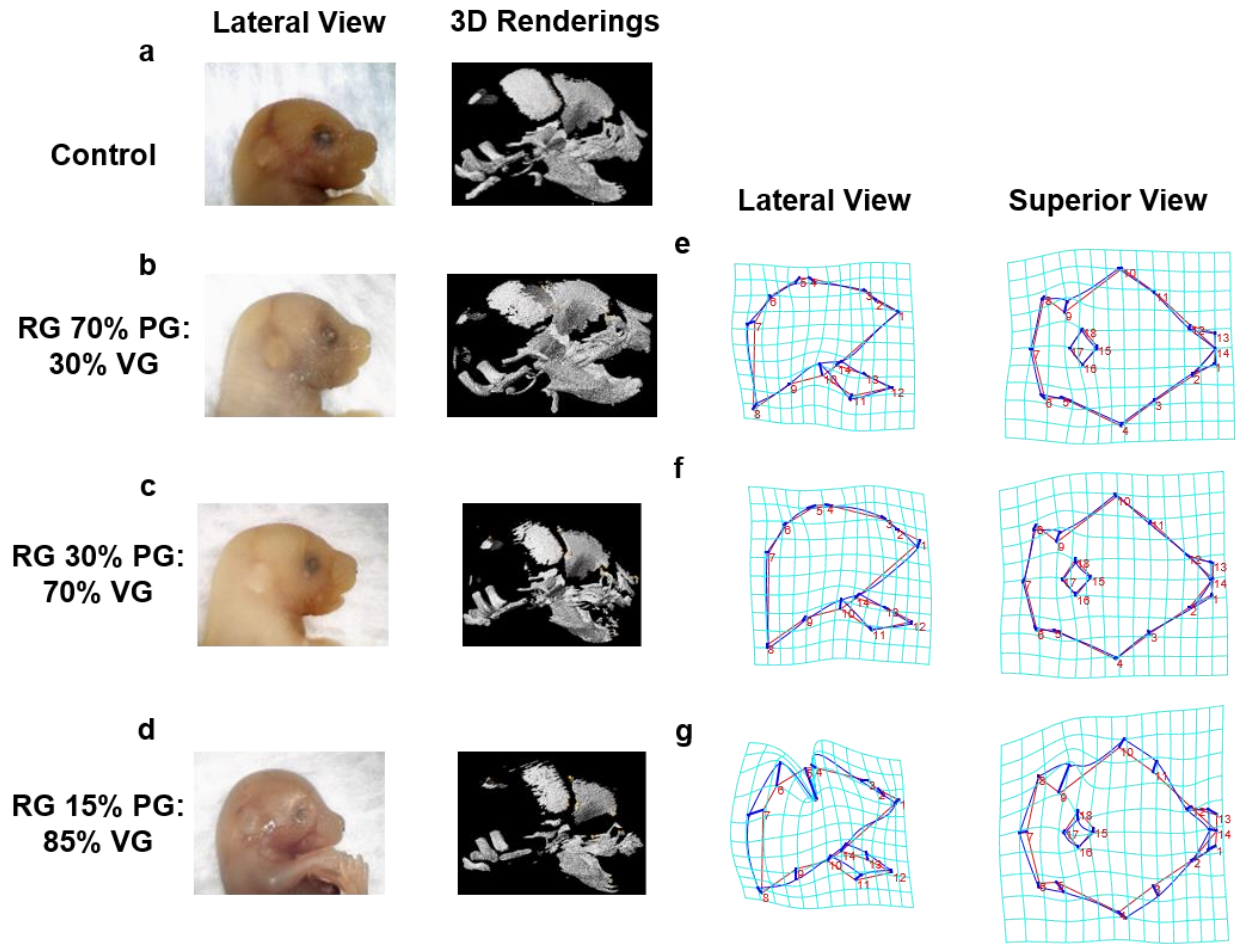

Figure 6: Unflavored e-cigAM exposure exhibits changes in shape morphology. (a-d) Light microscope images and 3D renderings of unflavored e-cigAM with various ratios of propylene glycol (PG) and vegetable glycerin (VG). (e-g) Transformation grids and wireframe overlays (red line represents control group and blue line represents treated group) for RG e-cigAM. Lateral and superior views were displayed.

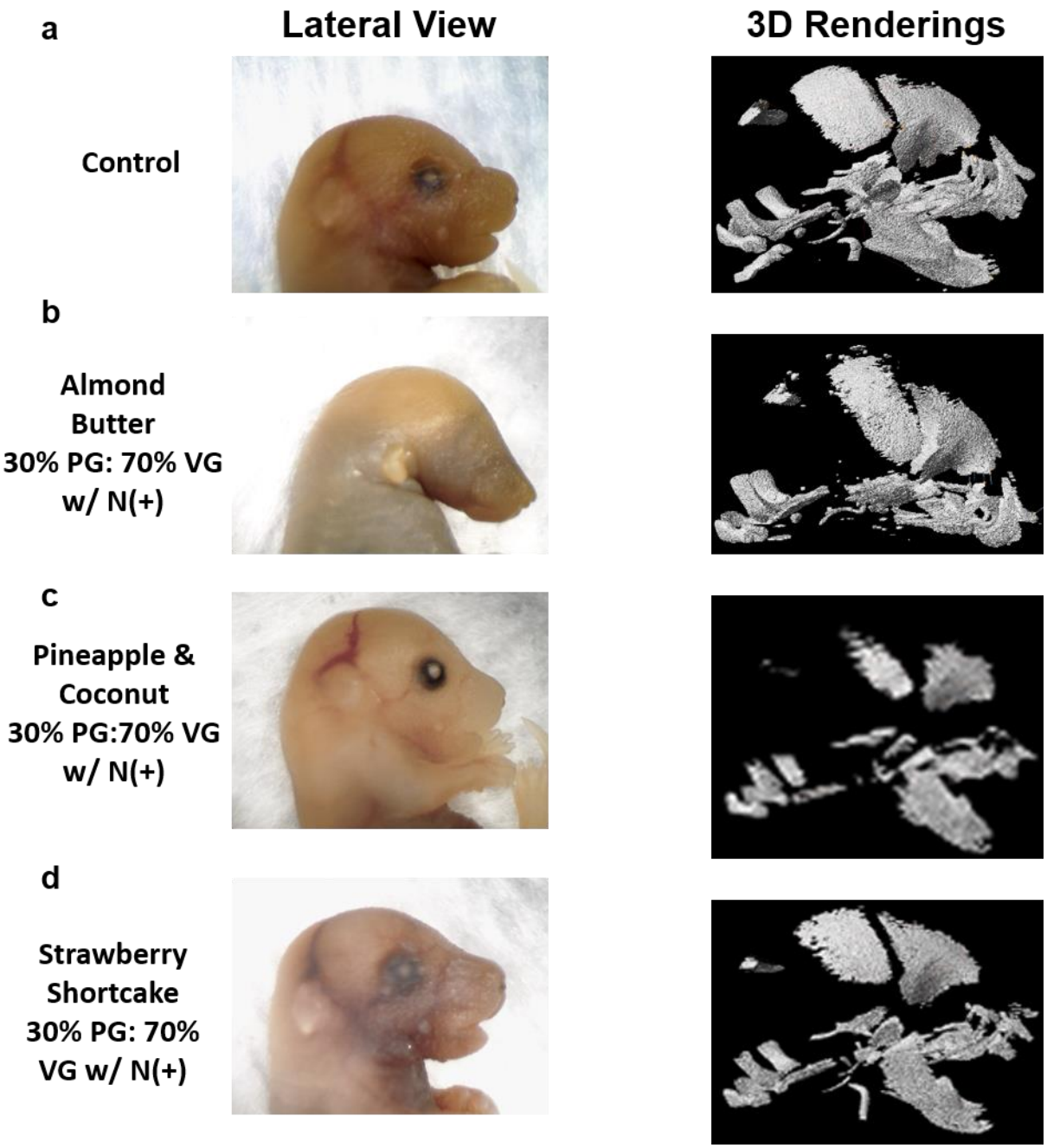

Figure 7: Flavored e-cigAM exposure exhibits changes in shape morphology. (a-d) Light Microscope images and 3D renderings of flavored e-cigAM with various ratios of propylene glycol (PG) and vegetable glycerin (VG.

Table 2. Landmark measurements of cranial vault bony features.

LM 1 – 8 describes the cranial vault bony features such as the frontal, parietal, occipital bones.

Vault Landmarks	Descriptions
LM 1	Intersection of frontal bone, lacrimal bone, frontal process of maxilla (left and right)
LM 2	Distance between most anterior point of premaxilla and most medial point on superior edge of occipital bone
LM 3	Distance between most superoposterior point of frontal bone and apex of mandibular process
LM 4	Distance between most anteroinferior point of mandible most anterior point of premaxilla
LM 5	Distance between most superior point of frontal bone (RIGHT) most superior point of frontal bone (LEFT)
LM 6	Distance between most lateral intersection of parietal and frontal bones, on frontal bone (RIGHT) and most lateral intersection of parietal and frontal bones, on parietal bone (RIGHT)
LM 7	Distance between most lateral intersection of parietal and frontal bones, on parietal bone (LEFT) and most lateral intersection of parietal and frontal bones, on frontal (LEFT)
LM 8	Length of superior aspect of occipital bone

Table 3. Landmark measurements of orofacial bony features.

LM 9 – 18 describes orofacial bony features such as the palatine foramen, premaxilla, zygoma, malar process, and mandible.

Orofacial Landmarks	Descriptions
LM 9	Distance between most anterior point in anterior palatine foramen (LEFT) most posterior point in posterior palatine foramen (LEFT)
LM 10	Distance most anterior point in anterior palatine foramen (RIGHT) most posterior point in posterior palatine foramen (RIGHT)
LM 11	Length of medial curvature of premaxilla (LEFT)
LM 12	Length of medial curvature of premaxilla (RIGHT)
LM 13	Length of zygoma (RIGHT)
LM 14	Length of malar process (RIGHT)
LM 15	Length of zygoma (LEFT)
LM 16	Length of malar process (LEFT)
LM 17	Length of superior aspect of mandible (RIGHT)
LM 18	Length of superior aspect of mandible (LEFT)

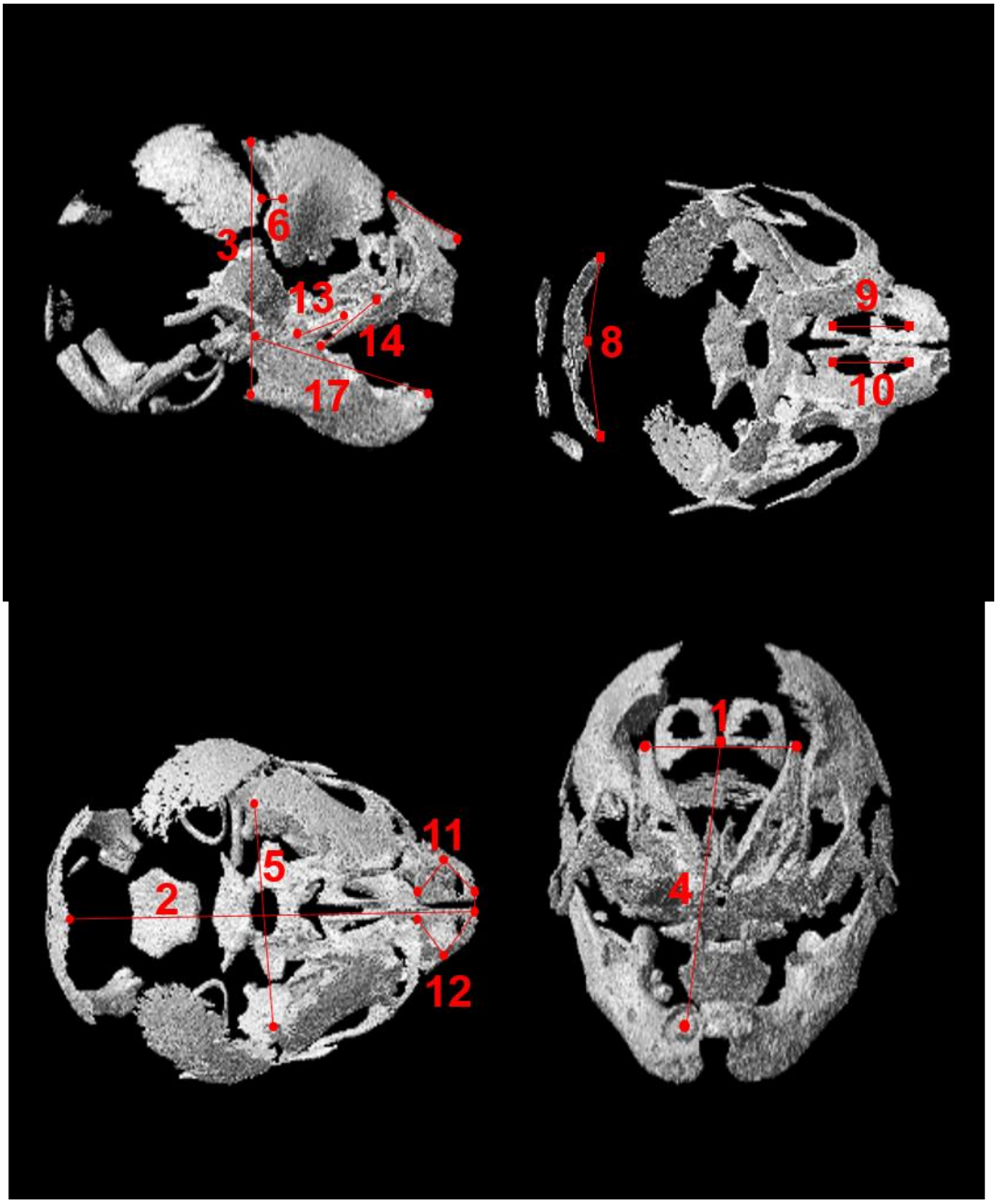

Figure 8: Placement of cranial vault and orofacial landmarks in 17.5E mouse embryos.
The absolute distance measurements were analyzed from twenty essential landmarks. Additionally, a total of 516 landmarks and semi-landmarks were placed on the frontal, parietal, baso-occipital bone as well for GM analysis.

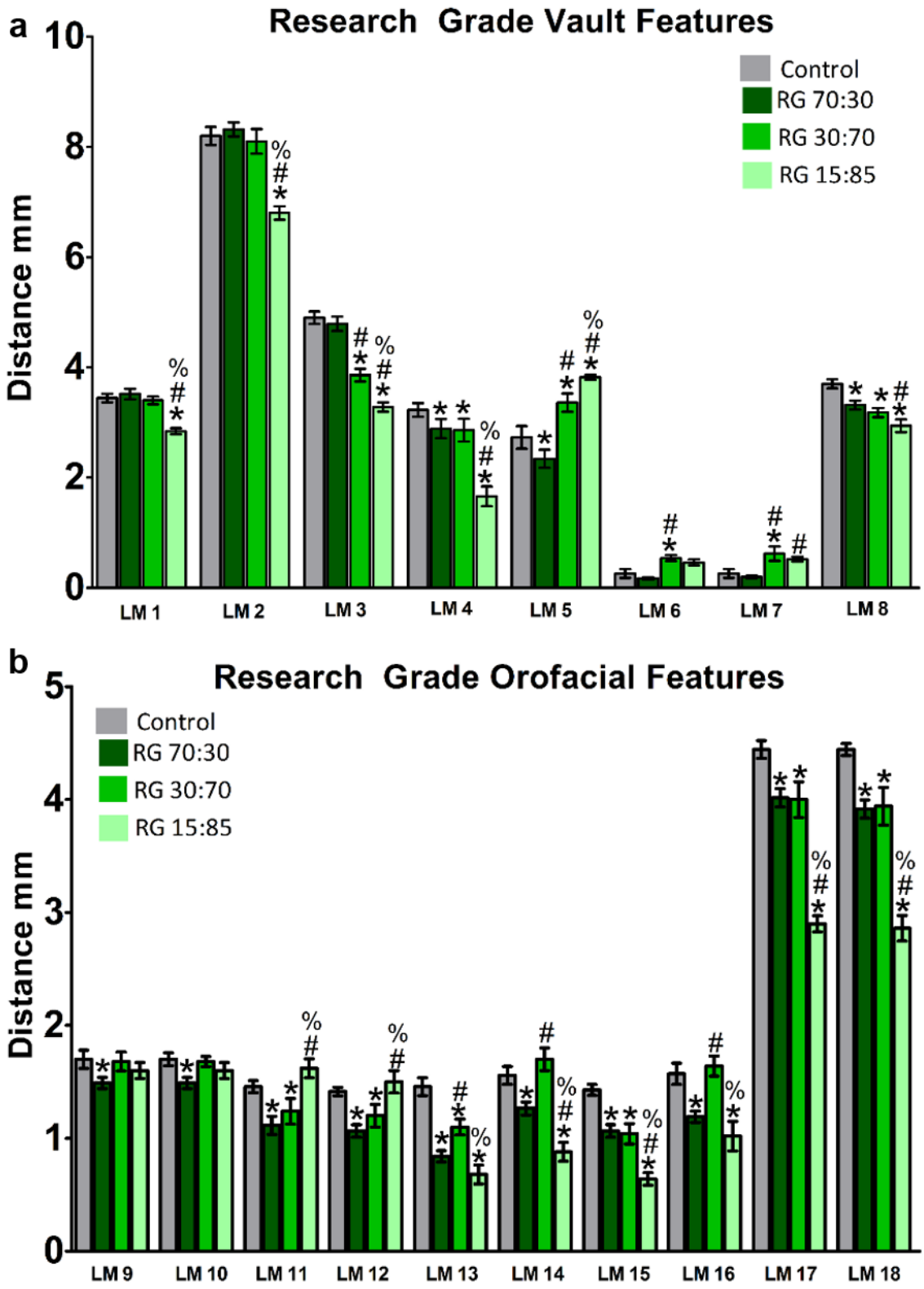

Figure 9: Research Grade e-cigAM quantitative changes in cranial vault and orofacial landmark measurements.

(a) Landmark measurements of research grade cranial vault bony features. RG 15/85 had significant changes in LM measurements compared to control/other PG-VG ratio RG e-cigAM. (b) Landmark measurements of research grade orofacial bony features. The pre-maxilla, zygoma, malar process, and mandible bones were most affected. * $p < 0.05$ vs. Control, # vs. RG 70/30, % vs. RG 30/70

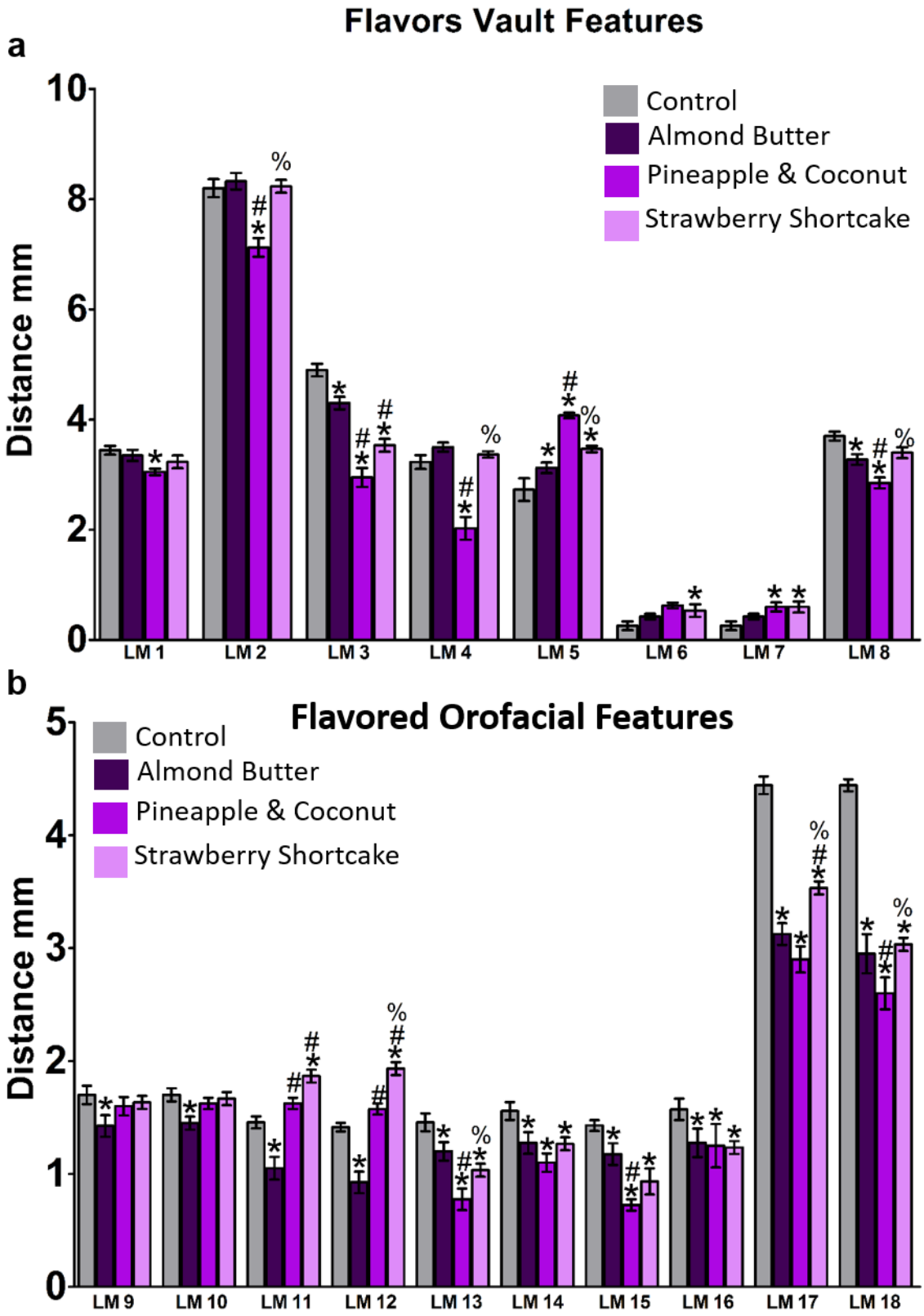

Figure 10: Flavored e-cigAM quantitative changes in cranial vault and orofacial landmark measurements.

(a) Landmark measurements of flavored cranial vault bony features. All three flavors had significant changes in LM measurements compared to control/other flavors. (b) Landmark measurements of flavored orofacial bony features. The pre-maxilla, zygoma, malar process, and mandible bones were most affected. * $p < 0.05$ vs. Control, # vs. Almond Butter, % vs. Pineapple and Coconut

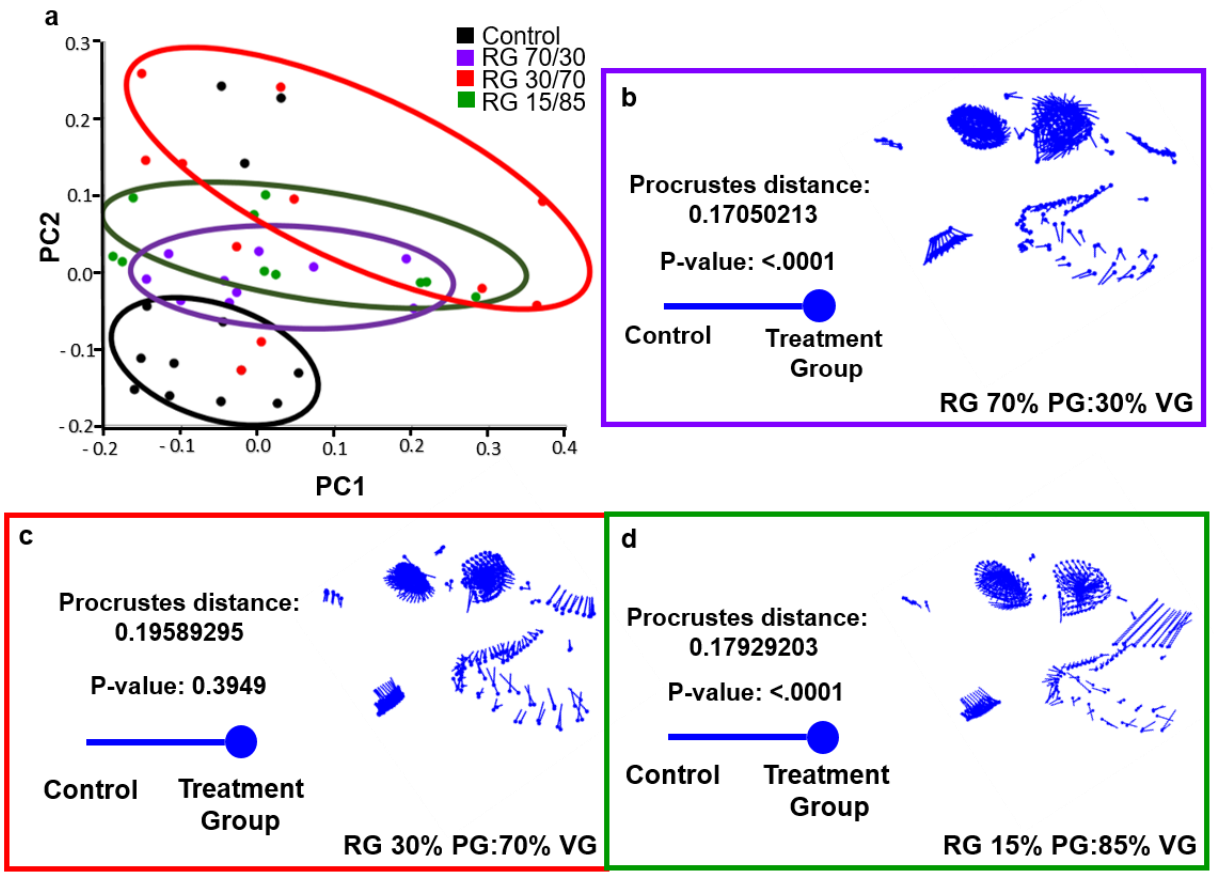

Figure 11: Geometric morphometric analysis of mice embryos exposed to RG e-cigAM. (a) A principal component analysis (PCA) was performed to illustrate shape changes within samples and ultimately groups as well. The first two principal components produced from the landmarks displayed over 50% of the variance within all groups. All groups were distinguished from each other in both PC1 and PC2, with PC2 being the most prominent. (b-d) A discriminant function analysis (DFA) was performed to illustrate shape changes within two groups, specifically a treated group (RG 70/30, 30/70, or 15/85) versus the control group. The most prominent areas that were affected were the nasal/snout area and the mandible region.

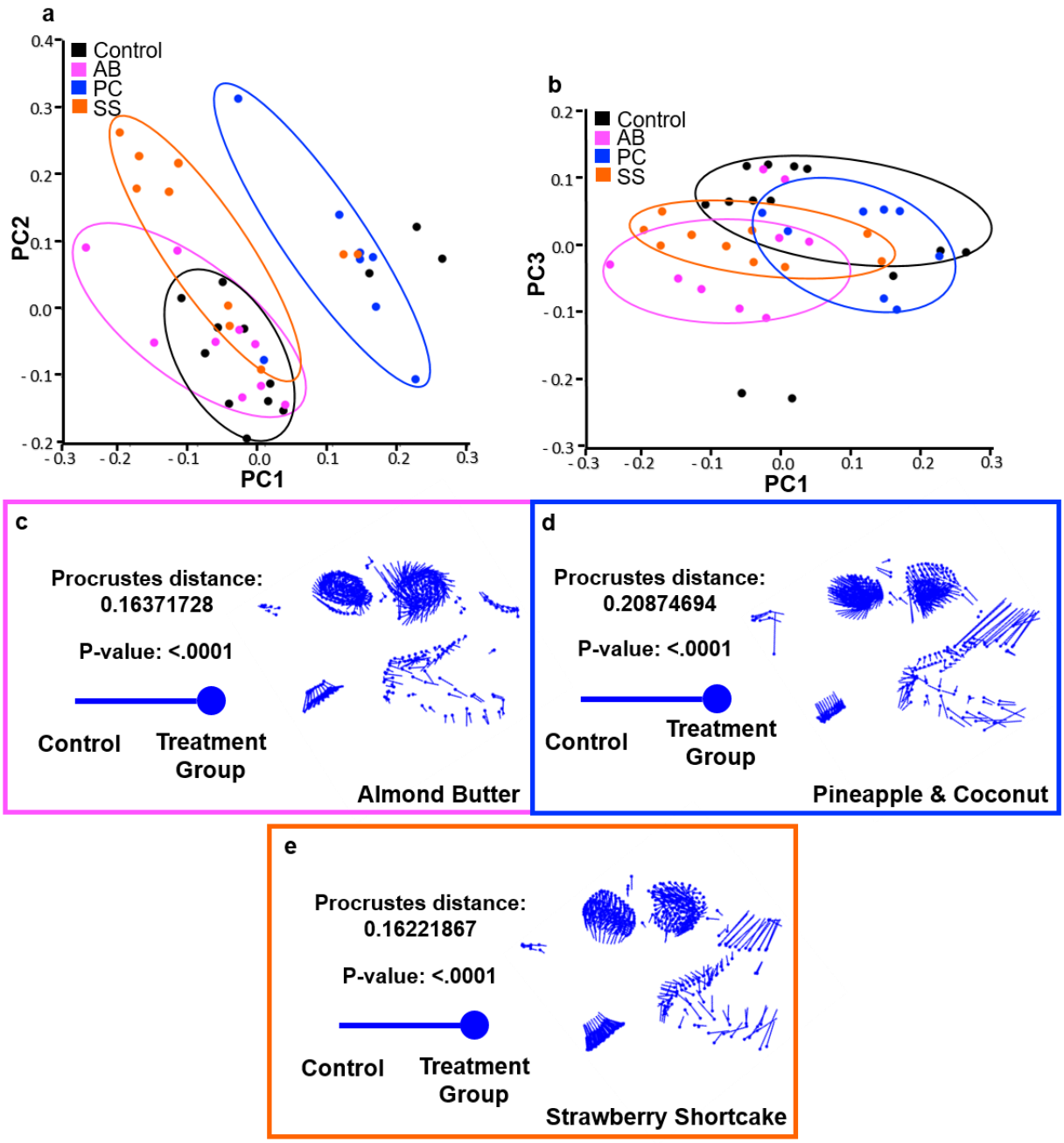

Figure 12: Geometric morphometric analysis of mice embryos exposed to flavored e-cigAM. (a-b) A principal component analysis (PCA) was performed to illustrate shape changes within samples and ultimately groups as well. The first three principal components produced from the landmarks displayed over 50% of the variance within all groups. All groups were distinguished from each other in both PC1, PC2, and PC3 with PC1 being the most prominent. (b-d) A discriminant function analysis (DFA) was performed to illustrate shape changes within groups, specifically a treated group (AB, PC, and SS) versus the control group. The most prominent areas that were affected were the nasal/snout area and the mandible region.

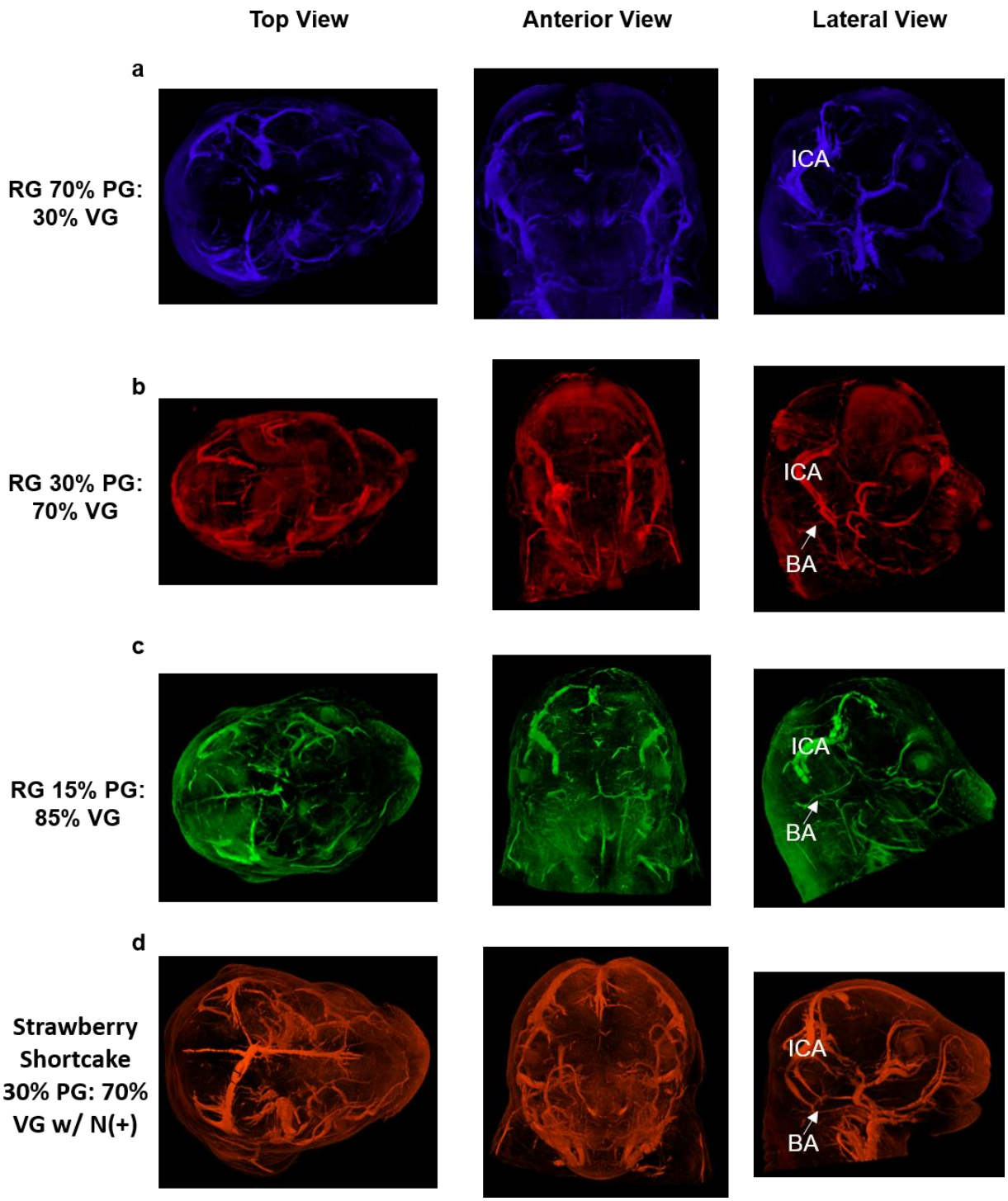

Figure 13: Qualitative analysis of blood vessels in Research Grade and flavored e-cigAM. (a-d) Maximum intensity projection (MIP) images of mouse embryos with iodine staining with all unflavored Research Grade e-cigAMs and one flavored Strawberry Shortcake e-cigAM. The major cerebral arteries were moderately visualized in most groups. Abbreviations: basilar artery, BA; internal carotid arteries, ICA;

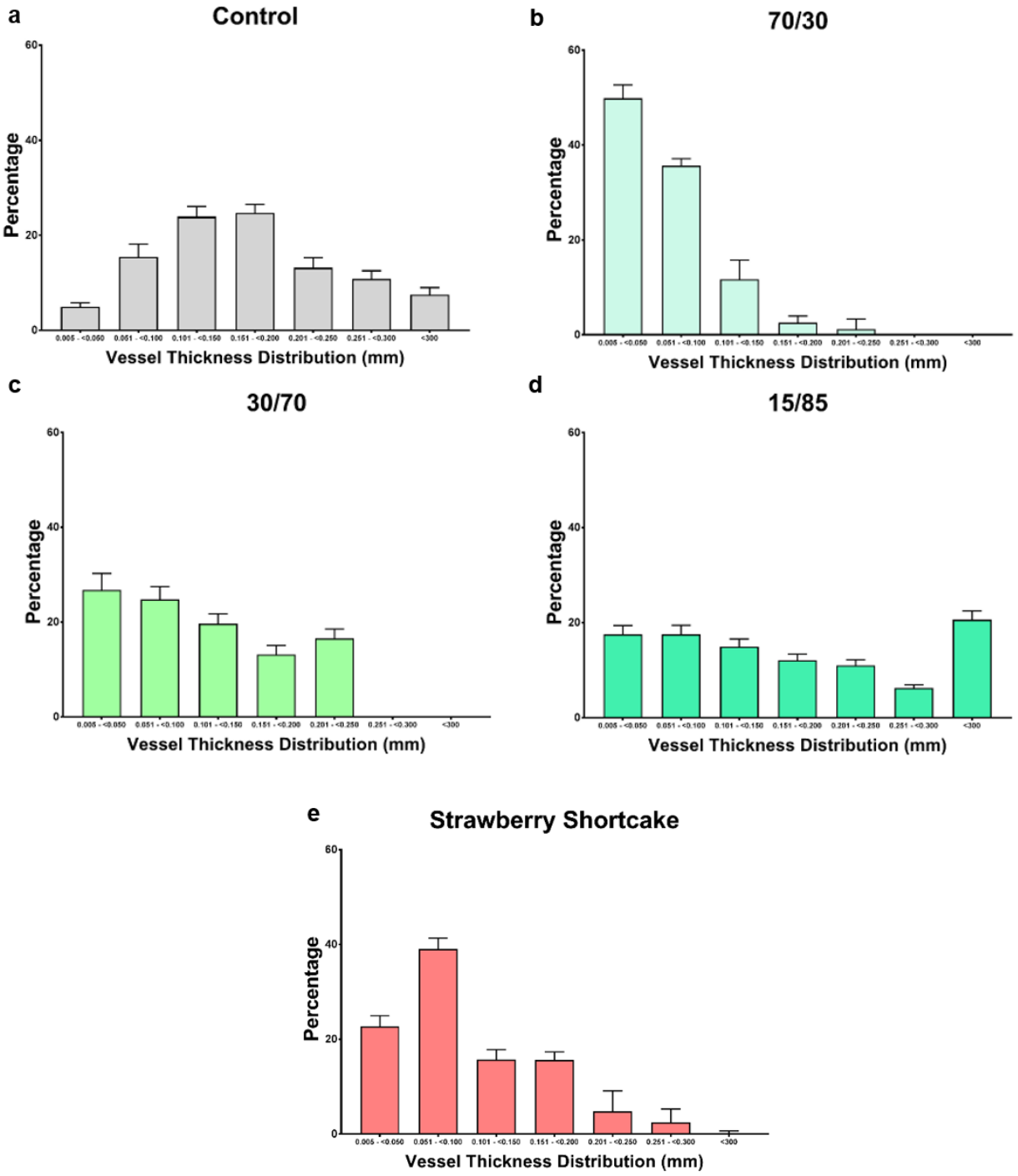

Figure 14: Vessel thickness distribution in e-cigAM exposed mice embryos via micro-CT analysis. (a-d) Quantitative analysis of the vascular network followed a similar method as histomorphometric trabecular/cortical bone architecture. The parameters that were analyzed included thickness distribution in RG 30/70, 70/30, 15/85, and Strawberry Shortcake. All graphs should be analyzed compared to the control.

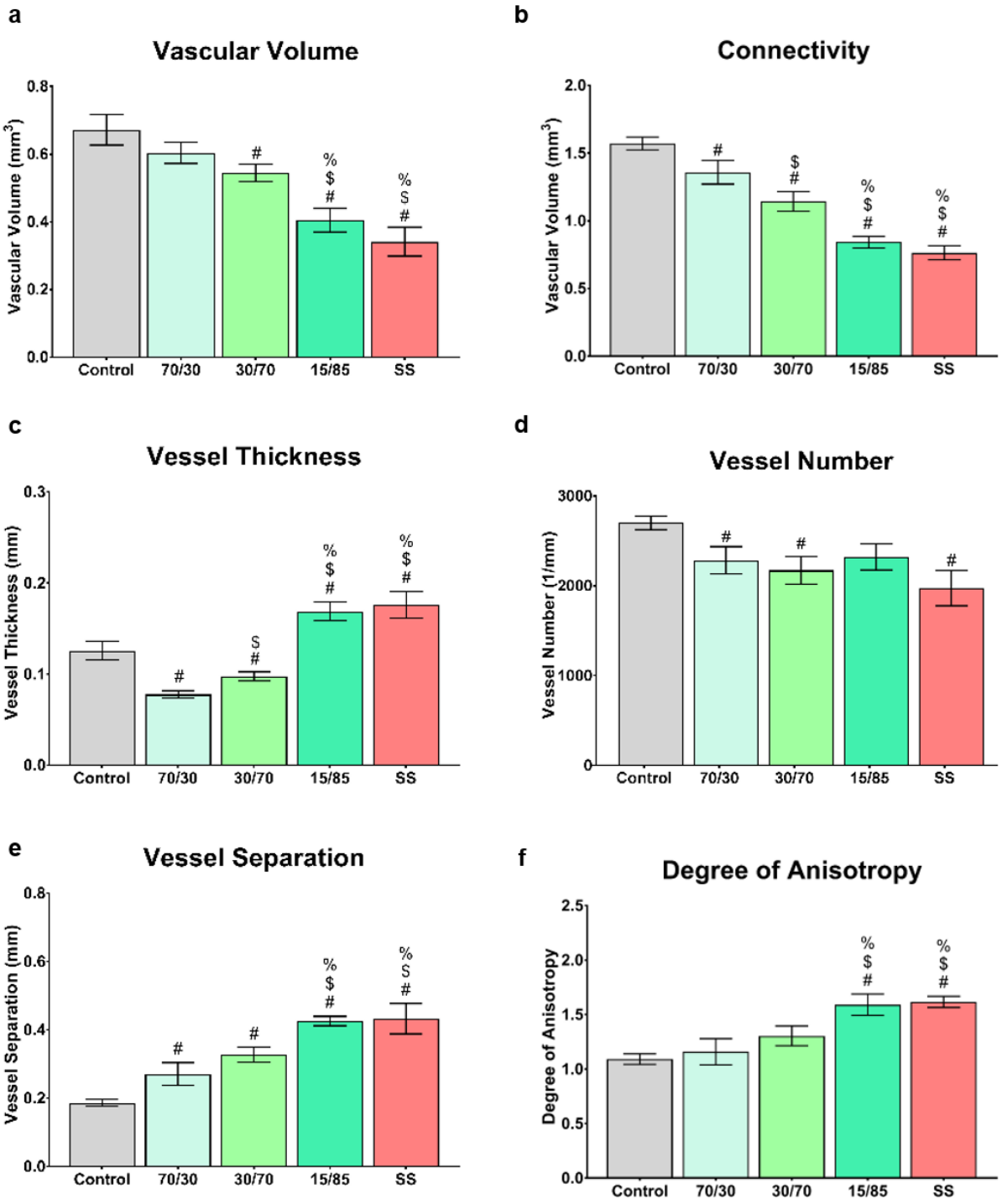

Figure 15: Quantitative micro-CT analysis of angiogenesis in e-cigAM exposed mice embryos showed a PG – VG ratio dependence. (a-j) Quantitative analysis of the vascular network followed a similar method as histomorphometric trabecular/cortical bone architecture. The parameters that were analyzed included thickness distribution (a-d), vascular volume (e), connectivity (f), thickness (g), vessel number (h), separation (i), and degree of anisotropy (j). # $p < 0.05$ vs. Control, $ vs. RG 70/30, % vs. RG 30/70

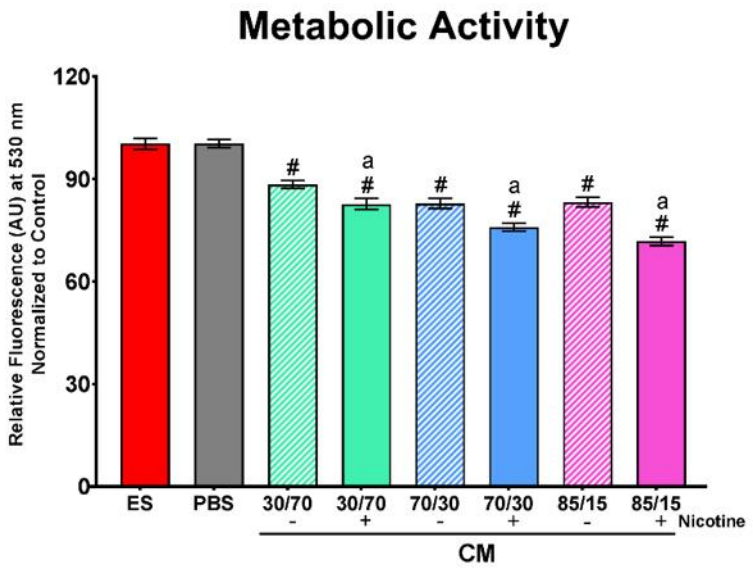

Figure 16: E-cigAM exposure on neural crest cell metabolism and viability. Three different VG/PG ratio groups were assessed ranging from 30/70, 70/30, and 85/15. Nicotine and no nicotine groups were also assessed for each VG/PG group. + indicates nicotine, and – indicated no nicotine. # $p < 0.05$ vs. PBS and ES, a vs. respective no nicotine group within each VG/PG group.

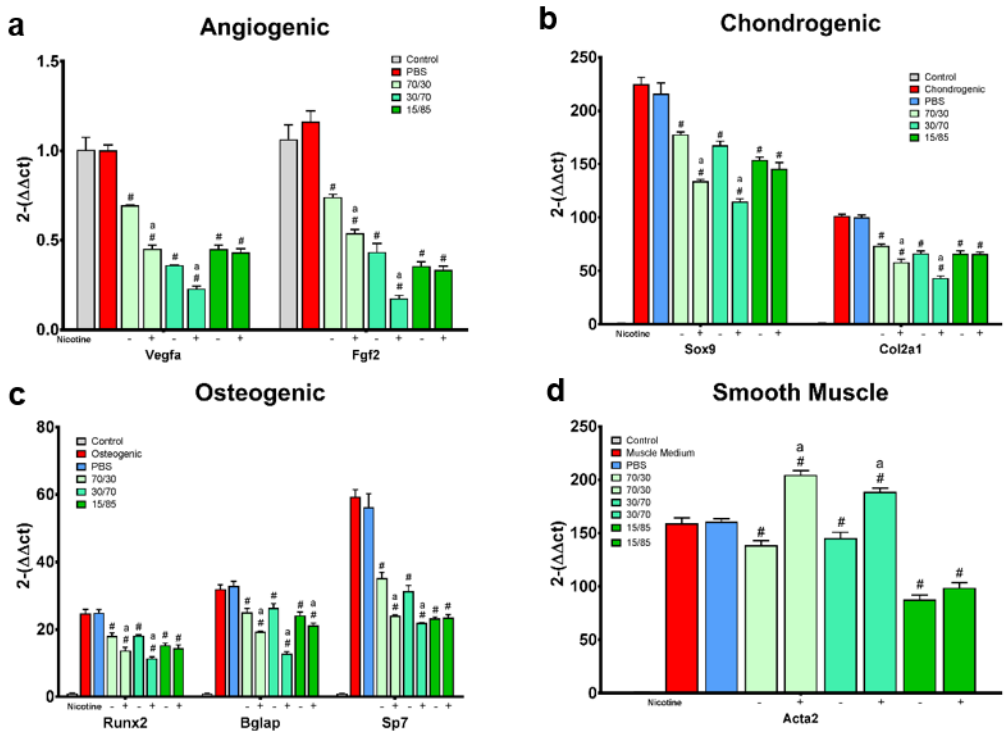

Figure 17: E-cigAM exposure attenuates the expression of genetic markers of NCC angiogenesis, chondrogenesis, osteogenesis and smooth muscle (a) Angiogenic differentiation was assessed using *Vegfa* and *Fgf2* markers. (b) Chondrogenic differentiation was assessed using *Sox9* and *Col2a1* markers. (c) Osteogenic differentiation was assessed using *Runx2*, *Bglap,* and *Sp7* markers. (d) Smooth muscle was assessed by *Acta2* marker +/- indicate the presence or absence of nicotine in each PG/VG group. # $p < 0.05$ vs. PBS, a vs. respective no nicotine group within each VG/PG group.

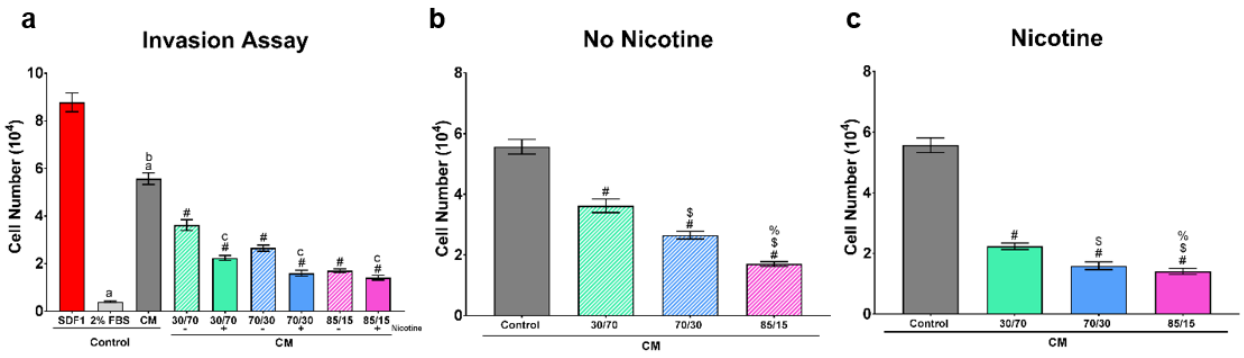

Figure 18: Neural crest cell migration was inhibited by e-cigAM dependent on VG/PG and nicotine ratio. (a) Exposure was decreased to all e-cigAM types (30:70 +/-, 70:30 +/-, and 15:85 +/-). (b) No nicotine e-cigAM types of 30:70, 70:30, and 15:85 showed a decrease in migration. (c) Nicotine e-cigAM types of 30:70, 70:30, and 15:85 preserved this decrease in migration but was enhanced. a $p < 0.05$ vs. SDF1, b vs. 2% FBS, c vs. respective no nicotine group within each VG/PG group, # vs. CM/Control, $ vs. 30/70, % vs. 70/30.

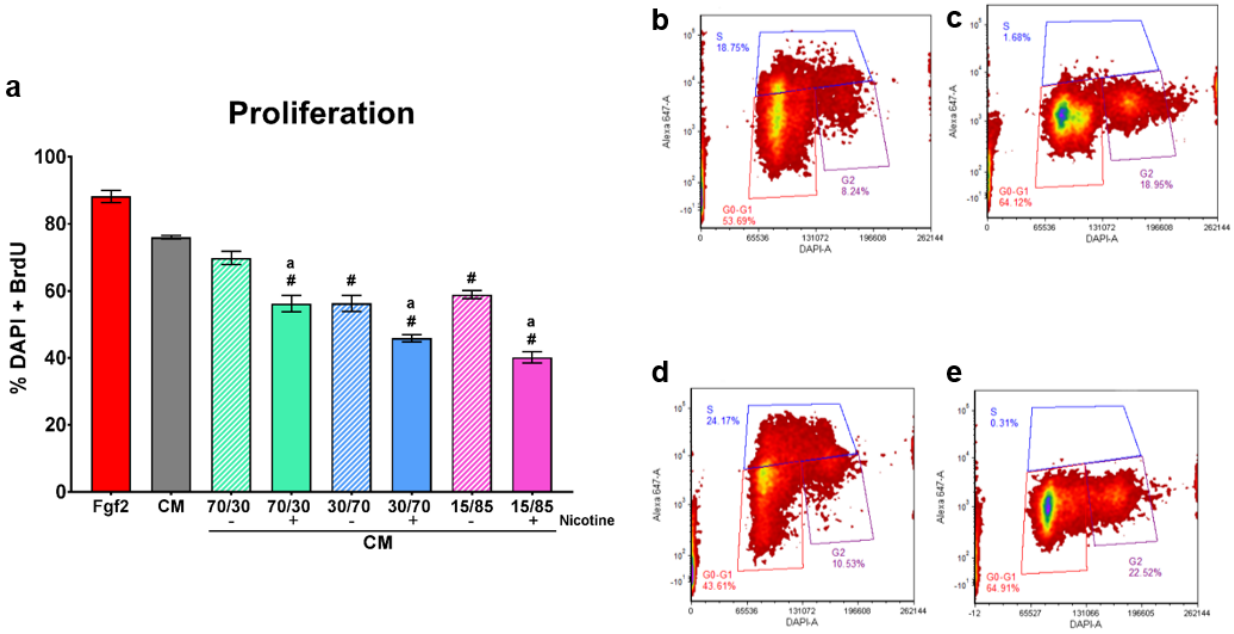

Figure 19: E-cigAM inhibits NCC proliferation dependent on PG/VG ratio and nicotine dependence. (a) Proliferation was decreased in all groups except for the 70/30- group. (b) Flow cytometric analysis with no fibroblast growth factor (FGF) showing G0-G1, S, and G2 phases of cell cycle. (c) Flow cytometric analysis with FGF showing G0-G1, S, and G2 phases of cell cycle. (d) Flow cytometric analysis of 15/85 PG/VG group with no nicotine showing G0-G1, S, and G2 phases of cell cycle. (e) Flow cytometric analysis of 15/85 PG/VG group with nicotine showing G0-G1, S, and G2 phases of cell cycle. # $p < 0.05$ vs. CM, a vs. respective no nicotine group within each VG/PG group.